Christof Wehmeyer

A Floating Offshore Wind Turbine in Extreme Wave Conditions

Revised Version

PhD Thesis defended at Aalborg University,
Department of Civil Engineering

River Publishers

A Floating Offshore Wind Turbine in Extreme Wave Conditions

A Floating Offshore Wind Turbine in Extreme Wave Conditions

Revised Version

PhD Thesis
Defended in public at Aalborg University
3 December 2014

Christof Wehmeyer

Department of Civil Engineering,
The Faculty of Engineering and Science,
Aalborg University, Aalborg, Denmark

River Publishers

ISBN 978-87-93237-40-7 (e-book)

Published, sold and distributed by:
River Publishers
Niels Jernes Vej 10
9220 Aalborg Ø
Denmark

Tel.: +45369953197
www.riverpublishers.com

CONTENTS

TABLE OF FIGURES

LIST OF FIGURES WHERE PERMISSION HAS TO BE GRANTED

(THIS EDITION IS NOT AN OFFICIAL PUBLICATION AND THEREFORE PERMISSION IS NOT NEEDED)

INCLUDED PAPERS

Appendix 1

Wehmeyer, C., Skourup J., Frigaard P. B. (2012). "Generic Hurricane Extreme Sea State. An engineering approach", Proc 22nd Int Offshore and Polar Eng Conf, Rhodes, ISOPE.

Appendix 2

Wehmeyer, C., Ferri, F., Skourup J., Frigaard P. B. (2013). "Experimental Study of an Offshore Wind Turbine TLP in ULS Conditions", Proc 23rd Offshore and Polar Eng Conf, Anchorage, AK, ISOPE.

Appendix 3

Wehmeyer, C., Ferri, F., Andersen M. T., Pedersen R. R., (2014). "Hybrid Model Representation of a TLP including flexible topsides in non-linear regular waves", Energies 2014, 7, 5047-5064; doi:10.3390/en7085047

Appendix 4

Wehmeyer, C., Rasmussen J. H. (2014). "Mooring responses of a floating offshore wind turbine in non-linear irregular waves", Journal of Ocean and Wind Energy (JOWE) 2014, (submitted)

GLOSSARY

AAU	*Aalborg University*
API	*American Petroleum Institute*
CFD	*Computational Fluid Dynamics*
CoE	*Cost of Energy*
COG	*Centre of Gravity*
DNV	*Det Norske Veritas*
DOF	*Degree of Freedom*
FOWT	*Floating Offshore Wind Turbine*
FEED	*Front End Engineering Design*
GOM	*Gulf of Mexico*
IRF	*Impulse response Function*
IFFT	*Inverse Fast Fourier Transform*
kV	*Kilovolt*
MW	*Megawatt*
MWh	*Megawatt hour*
NREL	*National Renewable Energy Laboratory*
OWT	*Offshore Wind Turbine*
POA	*Point of Attack*
QTF	*Quadratic Transfer Function*
RAO	*Response Amplitude Operator*
RNA	*Rotor Nacelle Assembly*
TB	*Tower Bottom*
TLP	*Tension Leg Platform*
TM	*Top Mass*
TWh	*Terawatt hours*
ULS	*Ultimate Limit State*

Greek Symbols

γ	*Spectral peak enhancement Factor*
ζ_1 & ζ_2	*Structural damping values for the first and second eigenmode*
η	*Wave elevation*
μ_{ij}^{COG}	*Radiation Damping Force vector at COG*
μ	*Transformed Radiation Damping Force vector at Point of Interest*

A	*Projected Area*
A_i *or* A_j	*Amplitude of the sinusoidal regular wave*
A,B,C,D	*State Space Matrices*
C_a	*Added Mass Coefficient*
C_D	*Drag Coefficient*
$C_{Topside}$	*Structural Damping Matrix of the Topside*
C_{ij}^{rad}	*Impulse Response Function of the Radiation Damping*
$F_{exc}(t)$	*1st order wave excitation Force in time domain from summation of sinusoidal components*
$F_i^{exc}(t)$	*1st order wave excitation Force in time domain from the convolution of non-causal IRF with*
$F_{exc}(\omega_i)$	*1st order wave excitation force coefficient in the frequency domain*
$F_{exc}^{Sum}(t)$	*2nd order wave excitation Force in time domain from summation of sinusoidal components*
$F_{exc}^{Sum}(\omega_i, \omega_j)$	*Complex sum frequency dependent 2nd order wave excitation coefficients*
$F_{exc}^{Diff}(t)$	*2nd order wave excitation Force in time domain from summation of sinusoidal components*
$F_{exc}^{Diff}(\omega_i, \omega_j)$	*Complex different frequency dependent 2nd order wave excitation coefficients*
$F_{Mooring}$	*Mooring Force Vector*
$F_{Exc\_inertial}$	*Excitation Force vector due to Diffraction Force and Froude-Krylov Force*
$F_{Exc\_viscous\ drag}$	*Excitation Force vector due to hydrodynamic viscous Drag*
g	*Acceleration of Gravity*
$H(r_{COG})$	*Transformation matrix from centre of gravity to point of interest*
h_i^{exc}	*Excitation force unit impulse response functions*
H_{max}	*Design Wave Height*
H_{m0}	*Spectral significant wave height*
H_s	*Statistical significant wave height, generally assumed equal to Hm0*
k_i	*wave number*
$K_{Topside}$	*Structural Stiffness Matrix of the Topside*
$K_{Floater}^{COG}$	*Hydrostatic Stiffness matrix of the Floater at COG*
$K_{Floater}$	*Transformed hydrostatic Stiffness matrix of the Floater at Point of Interest*
l	*Length of the Tower*
$M_{Floater}^{COG}$	*Mass matrix of the Floater at COG*
$M_{Floater}$	*Transformed Mass matrix of the Floater at Point of Interest*
$M_{Topside}$	*Mass Matrix of the Topside*
M_{Tower}	*Mass matrix of the Tower*
$mh_{Floater}^{COG}$	*Hydrodynamic added Mass matrix of the Floater at COG*

ρ	*Density*
φ_i	*Random phase*
ω_i	*Wave frequency of the ith Wave*
ω_1 & ω_2	*1st and 2nd structural eigenfrequencies of the topside*
$mh_{Floater}$	*Transformed Hydrodynamic added Mass matrix of the Floater at Point of Interest*
T_{Design}	*Period of Design Wave*
T_p	*Peak Wave Period*
r_{COG}	*Vector from COG to Point of Interest*
SF30	*30th order Stream-function Wave*
u	*water particle velocity*
v	*small body of mass velocity*
V	*small body Volume*
x	*Displacement*

ACKNOWLEDGEMENT

THX to a lot of people for their patience, energy, advices and support.

Eva
Ella
Mom
Dad
Arnold
Gitte
Anne
Morten
Gry
Johannes
Lærke
Cecilie
Svenna
Riten
Jona
Ronnie
Jørgen
Jesper
Peter
Thomas
Lars
Michael
Aurélien
Harry
Andrew
Cesco
Little John
Erf
Bernd
Eric
Baumänsche
Denis
Volkert
Moio
Klaus
Tim
Alexander
Mohsen
Sven
Verena
Peter
Gabi
Charlie
Judith
Hamish
Jason

Danish Ministry of Higher Education and Science,
AAU, Ramboll Offshore Wind,
Glosten Associates

1. EXECUTIVE SUMMARY & CONCLUSIONS

While the design of floating offshore wind turbines (FOWT) is still at an infant stage, the general desire to realise them is strong. According to a poll conducted by GL Garrad Hassan at the HUSUM 2012 Wind Energy Trade Fair, 62% of the attendees believed that floaters will be a part of the mix and will even overtake bottom fixed foundation within the coming two decades, Bossler (2011). FOWTs are believed having a large potential of lowering the cost of energy (CoE). The CoE minimization is currently the main driver for technological development in the offshore wind industry. Therefore reliable and purposes oriented design procedures are the backbone of a cost efficient offshore wind industry. Conventional engineering procedures for the assessment of extreme event impacts, i.e. ultimate limit state (ULS) analysis of floating structures, as they have been used in the oil and gas industry, neglect two important aspects, which make them non-conservative in use for FOWT:

(A) The offshore wind industry intends to install floating structures at much lower water depth (from 50m onwards), than the offshore oil & gas industry (from 300m onwards). In such cases a linear wave theory approach might not be sufficient to describe realistic wave shapes and the respective loads, especially in ULS conditions. In shallow or intermediate water depth environments, i.e. when the ratio between the water depth and the wave length becomes smaller than 0.5, waves need to be described by non-linear approaches, in order to account for their vertical asymmetry.

(B) Wind turbines are dynamically sensitive structures, i.e. while the floating part can be assumed more or less rigid – the flexibility of the slender tower supporting a heavy and very dynamic rotor-nacelle assembly influences the global structure's response significantly, especially in the pitch and roll degrees of freedom for taut moored systems.

The current work evaluates the performance of engineering procedures, used in the design of bottom fixed offshore wind turbines, for the hydrodynamic ULS analysis of a FOWT tension leg platform (TLP). Dynamically sensitive topsides are included and water depths are considered, where wave shapes in the extreme sea states deviate from the 1st order description. In detail the industrial PhD project comprises four work packages:

1. The author develops a design basis, which defines the hydrodynamic environmental design parameters. The aim is to define a sensible set of extreme sea state parameters, i.e. H_{m0}, T_p and peak enhancement factors, based on cyclonic storm conditions (see Wehmeyer et al. (2012), in Appendix 1).

2. Based on Wehmeyer et al. (2012), the author drafts a physical model test campaign considering the available facilities in the University of Aalborg. The author develops and leads the construction of a physical model based on an industry inspired floater design, which was provided to the author by a befriended designer (see Wehmeyer, (2013) et al., in Appendix 2).

3. Towards the background of the obtained observations from Wehmeyer et al. (2013), the author develops a numerical model. A comparison of measured pitch responses versus the numerically predicted pitch responses, as well as a code to code comparison in regular non-linear waves serves as initial key performance indicator and good agreement is found (see Wehmeyer et al. (2014), in Appendix 3).

4. As a final step, the author extends the previous model in order to include non-linear irregular incident waves as well as non-linear irregular incident waves with an embedded Stream-function wave. A linear background sea state into which a Stream-function wave is embedded is assumed no longer appropriate. Therefore a 2nd order sea state model is developed by the author and served as well as the background sea state in which the Stream-function wave was embedded. The combined sea state is then applied in the numerical model in order to investigate the bow tendon responses of the FOWT

TLP. A comparison of measured bow mooring responses and the numerically predicted bow mooring responses serves as key-performance-parameter (see Wehmeyer and Rasmussen (2014), in Appendix 4).

The TLP is equipped with an open source tower and rotor-nacelle-assembly equivalent based on the well-known NREL 5MW turbine, (Jonkman et al, 2009). An important aspect of the study is that it does not intend to verify a design. The industry inspired floater is designed for a water depth of around 100 meters and the respective tendon length was modelled to its full extent, physically as well as numerically. The waves however, are generated on a water depth that equals a prototype water depth of 56 meter. A redesign of the structure itself to the intended water depth is outside of the scope. However, the above circumstances allow a qualitative assessment of the numerical approaches to assess the behaviour of an FOWT in non–linear waves. This is also the reason, why actual measured values are only given as ratios.

The respectively developed numerical representation of the floating structure is a hybrid model that considers linear radiation damping and added mass and linear diffractive wave excitation together with non-linear viscous wave excitation by Morison's type loads, in order to include the wave nonlinearities. It is obvious that such an approach violates the linear potential theory assumptions and the degree of conservatism in terms of ultimate limit state design parameters (e.g. mooring loads) is unknown. Consequently a physical model test campaign is part of the current work in order to validate and benchmark the hybrid model. It is found, that the vertical asymmetry of the measured waves is numerically well covered by a 2nd order irregular sea state realisation. The physical wave realisations show maximum waves, of which one is an expected maximum wave in accordance with a Rayleigh distribution. The maximum waves are numerically represented by embedded Stream-function waves.

The author compares the resulting bow tendon loading of the hybrid model to the measured responses, as a key performance indicator. 90% to 95% of the loads show a satisfying match, though the hybrid model over predicts the remaining 5% to 10% maximum loads by 32%, 34% and 29% for a linear irregular sea state, a nonlinear irregular sea state and a nonlinear irregular sea state with an embedded Stream-function wave, respectively.

The limited number of sea states during the model tests as well as some model degradation during the physical testing campaign may cause some uncertainty of the measurements. However, based on the current status, it can be concluded that the non-linear wave embedded in a non-linear irregular background sea state provides the most controlled measure to assess critical ULS events for FOWT. The approach is similar to current state of the art ULS analysis of bottom fixed offshore wind turbines. So far it has however not been applied in floating structure designs, and the respective performance was unclear. The method is thought to be useful investigating the ultimate loading, high frequency responses from extreme transient effects and/or slack line events especially for TLP structures.

The differences between the hybrid model results and the observations highlight the need for further optimization and the consequent potential to make FOWT cost competitive. Generally the study shows that the hybrid modelling approach might currently be sufficient for pre-Detailed Design stages, where higher degrees of conservatism are acceptable. However for multi-unit production the current method includes a too high degree of conservatism and requires further improvement. The presented work summarizes the current status and should be understood as a basis for subsequent developments by highlighting the challenges in FOWT ULS design.

It is proposed to extend the current work by:

- Increasing the number of model tests with focus on ULS behaviour in intermediate to shallow waters.
- Increase the numerical model complexity by including the 2nd order inertial forces by quadratic transfer functions or by the instantaneous non-linear Froude-Krylov force.
- Sensitivity study on Stream-function wave embedment parameters.
- Investigate different substructures in order to understand the general applicability.

2. EXECUTIVE SUMMARY & CONCLUSIONS, PÅ DANSK

Til trods for at design procedurerne for flydende offshore vindmøller (Floating Offshore Wind Turbine, FOWT) endnu er i den tidlige udviklingsfasen, så er det generelle ønske i industrien, at flydende koncepter realiseres. Ifølge en meningsmåling udarbejdet af GL Garrad Hassan i HUSUM 2012 Wind Energy Trade Fair mente omtrent 62 % af deltagerne at flydende vindmøller bliver en realistisk løsningsmulighed og endda i løbet af 2 årtier også bliver den foretrukne løsning i stedet for funderingsløsninger, som installeres på havbunden, Bossler (2011). Det er den generelle overbevisning, at FOWTs kan minimere Cost of Energy (CoE). I øjeblikket styres den teknologiske udvikling i offshore vindbranchen primært af nedskrivningen af Cost of Energy (CoE). Derfor er pålidelige ingeniørmæssige procedurer nødvendige for at opnå kosteffektive løsninger. De konventionelle ingeniørmæssige procedurer til analyse af ekstreme hændelser (Ultimate Limit State, ULS) for flydende olie og gas konstruktioner tager ikke højde for to væsentlige forhold:

(A) Offshore vindindustrien planlægger at installere flydende strukturer på betydeligt lavere vanddybder (>50m) sammenlignet med olie og gas strukturer, som typisk installeres på større vanddybder (>300m). I tilfælde med lave vanddybder vil den lineære bølgeteori ikke være tilstrækkelig til at beskrive bølgekinematikken og de afledede belastninger specielt i tilfælde med ULS. Derfor er det nødvendigt at benytte ikke-lineære bølgemodeller for at forbedre beskrivelsen af det fysiske problem. Når forholdet mellem vanddybden og bølgelængden er mindre end 0,5 kan bølgerne ikke antages at være dybtvandsbølger, fordi bølgerne bliver vertikalt asymmetriske.

(B) Vindmøllekonstruktioner er generelt følsommer over for dynamiske påvirkninger, mens den flydende konstruktion under samme forhold kan betragtes som et stift legeme. Fleksibilitet i det slanke vindmølletårn, som understøtter en relativ tung rotor og nacelle påvirker i væsentligt grad det globale systems respons specielt i pitch og roll frihedsgraderne i forspændte systemer.

Denne afhandling evaluerer på de ingeniørmæssige procedurer, som i dag bruges til design af fundamenter installeret i havbunden og om hvorvidt disse procedurer kan anvendes til ULS analyser af FOWTs tension leg platform (TLP). Vanddybder, hvor bølgeformerne afviger fra første ordens bølgeteori, er inkluderet i analyserne ligesom indflydelsen fra den dynamisk følsomme konstruktion. Denne afhandling er opdelt i 4 work packages:

1. Der udvikles en design basis, som definerer de hydrodynamiske design parametre, hvor meningsfulde parametre til beskrivelse af de ekstreme søtilstande fastlægges, det vil sige, H_{m0}, T_p og Peak enhancement faktorer, som er baseret på cykloniske storme (se Wehmeyer et al. (2012)).

2. Med udgangspunkt i Wehmeyer et al. (2012) defineres en række fysiske modelforsøg, hvor faciliteterne på Aalborg Universitet benyttes. Forsøgsmodellerne er opbygget med inspiration fra et industrielt projekt med flydende strukturer, hvor selve designet er stillet til rådighed af anden konsulent virksomhed (se Wehmeyer et al. (2013)).

3. Baseret på forsøgsdata opstilles en numerisk model, der muliggør en sammenligning af pitch bevægelser fra forsøg og simuleringer og en sammenligning med resultater fra ANSYS AQWA for regulære ikke-lineære bølger, hvor en god overensstemmelse er påvist (se Wehmeyer et al. (2014)).

4. Den numeriske model udvides til også at inkludere ikke-lineære irregulære bølger og ikke-lineære irregulære bølger med en overlejret strømfunktionsbølge, da lineære irregulære bølger ikke repræsenterer forsøgsdata tilfredsstillende. Derfor er en anden-ordens søtilstand udviklet med en overlejret strømfunktionsbølge. Den kombinerede søtilstand anvendes i den numeriske model, hvor bovforankringslaster af den FOWT TLP nu kan simuleres. En sammenligning af målte og simulerede bovforankringslaster er et nøgletal til at beskrive performance af den numeriske model (se Wehmeyer and Rasmussen (2014)).

TLP modellen er udstyret med en akademisk open source vindmøllemodel (NREL). Den industri-inspirerede FOWT er designet til en vanddybde omkring 100 meter og de tilhørende forankringslængder er modelleret både i de fysiske forsøg og i den numeriske model. Derimod er bølgerne genereret på en vanddybde, der til svarer en vanddybde på 56 meter i prototype-dimensioner. Et re-design af strukturen for den planlagte vanddybde er uden for emnet af denne afhandling, men de ovenstående resultater gør det muligt at give en kvalitativ eftervisning af de numeriske modeller for analyser af en FOWT i ikke-lineære bølger. Dette er også grunden til at de faktiske måleresultater ikke er angivet men alene forholdstal er benyttet.

De respektive udviklede numeriske modeller anvender en hybridmetode baseret på hydrodynamiske koefficienter fra potentialteori og Morison laster for på den måde at kunne inkludere den ikke-lineære bølgekinematik. Det er en kendsgerning, at denne metode er i modstrid med potentialteoriens antagelser og graden af konservatisme i ULS designet er ukendt. Derfor skal hybridmodellen valideres med resultater fra fysiske modelforsøg. Den vertikale asymmetri fra de målte bølger er simuleret tilfredsstillende med en numerisk 2. ordens irregulær realisation af søtilstanden. De målte bølger inkluderer den maksimale bølge, som kan forventes fra en Rayleigh-fordeling, som er repræsenteret i den numeriske bølgemodel med en overlejret strømfunktionsbølge.
Forfatteren sammenligner bovforankringslaster i hybrid modellen med målte værdier som en nøgleparameter. 90 % til 95 % af lasterne viser en tilfredsstillende overensstemmelse selvom modellen overestimerer de restende 5 % til 10 % maksimale laster med 32 %, 34 % og 29 % for henholdsvis lineære regulære bølger, ikke-lineære irregulære bølger og ikke-lineære irregulære bølger overlejret med en strømfunktionsbølge.

Det afgrænsede antal søtilstande, som er inkluderet i modelforsøgene og den generelle degradering af forsøgsmodellen igennem forsøgsperioden giver anledning til usikkerheder i de målte data. Det kan stædigvæk konkluderes baseret på de nuværende resultater, at ikke-lineære irregulære bølger overlejret med en strømfunktionsbølge er den bedste metode til at beskrive den kritiske ULS hændelse for en FOWT. Denne metode anvendes på tilsvarende måde i ULS design af vindmøllefundamenter installeret i havbunden, men det er nu også bekræftet, at metoden kan anvendes for flydende strukturer på lave vanddyder, hvilket var uklart før dette arbejde. Metoden tænkes anvendt til at undersøge ekstreme belastninger, høj frekvente påvirkninger fra ekstreme transiente effekter og "slack-lining events" i forankringer specielt for TLP strukturer. Forskellene mellem resultater fra den numeriske hybridmodel og eksperimentelle observationer påviste en nødvendighed for optimering, men samtidig også et stort potentiale til at gøre FOWT til en konkurrencedygtig løsning.

Generelt viser resultaterne fra denne afhandling, at den nuværende hybridmodel er tilstrækkelig til pre-Detailed Design, hvor konservative løsninger kan accepteres. Men de numeriske metoder kræver forbedringer, hvis de skal anvendes til at designe strukturer til masseproduktion.

Forslag til videre arbejde:

- Udbygge antallet af modeltest med fokus på ULS-analyser på mellemdybt til lavt vand
- Udbygge kompleksiteten af den numeriske model med andenordens-inertikræfter med kvadratiske transferfunktioner eller med ikke-lineær Froude-Krylov kræfter
- Følsomhedsanalyser af inklusionen af strømfunktionsbølgen i den irregulære bølgeserie
- Undersøgelse af forskellige substrukturer for at forstå den generelle anvendelse

3. NON-TECHNICAL PROJECT CONTEXT

By the time of project finalization this industrial PhD is the first of its kind carried out in the Offshore Wind Energy Department of Ramboll. The scientific knowledge as well as the organisational experiences made are invaluable and have been utilized within the host company already. The theoretical work was mainly carried out at the host company in Esbjerg, whereas the laboratory work was carried out at the University in Aalborg (AAU). Consultation with academic colleagues at AAU was mainly being done by electronic communication, due to the distance, but as well through bimonthly personal meetings at AAU. Invaluable knowledge was provided concerning floating structures and numerical modelling thereof by the host university. The network and open source culture at the AAU allowed quick solution access when facing obstacles. An international group of experts working in the field have inherited the cooperative atmosphere from the AAU civil engineering department, and several fruitful discussions have contributed to the progress of the project. Due to the future oriented scope of the project, the day-to-day consultancy work at the host company was only scarcely related to the project. That imposed challenges on time and resource planning, which were however overcome by a high degree of flexibility within the host company.

The project is also the first of its kind for the host university and a follow-up project has been initiated; a further PhD on FOWT. The project is a pacemaker for further research projects and thereby starting a new research area for the civil engineering department of the Aalborg University. The continuation of the collaborative work between the host company and the university on this specific subject will ensure mutual benefits and thereby continued optimization of the solution. The latter is one piece of the puzzle for achieving the current top target of the Offshore Wind Industry, i.e. to reduce the cost of energy by 30%-40%, and subsequent compliance with the 2050 goals and continued employment creation.

4. INTRODUCTION

Considering that the total EU energy consumption is around 3000TWh/annum, only 30% of the total available wind energy resources need to be utilized to fully satisfy demand (see Figure 1). It can be seen that 70% of the resources are in water depth greater than 50m, which is currently the anticipated threshold value for the transition between bottom fixed and floating structures, (Thiagaran and Dagher, 2014).

The current cost of (bottom fixed) offshore wind energy is around 150€/MWh. The target for any technology, i.e. bottom fixed as well as floating substructures, in 2020 is to be below 100 €/MWh. The focus of the past years has been steel saving on a turbine location specific foundation design level. For Ramboll Offshore Wind alone that results in more than 1000 individually designed, fabricated and installed monopile foundations. The current development is concerned with the development of deep water monopile foundations, i.e. so called XXL monopiles suitable for water depth up to 50m. However when supporting turbines of 8MW to 10 MW, the monopile will most probably reach its depth limits and currently proposed jacket solutions are 3-4 times more expensive than monopiles per weight unit, due to their complex construction and installation methods. Hence there is a need for industrialized deep water foundations, where standardization is crucial. Currently foundations need to be of high precision and have very low fabrication tolerances. It has been the experience that such high quality is challenging to be obtained outside of Europe. Floaters, however, can be produced on a turbine or wind farm specific level and in the same instance accommodate much higher fabrication tolerances, which enables a standardized production in less expensive facilities. The history of ship yards and ship building has shown that it is much cheaper to build floating structures outside of Europe.

Another keyword of the future is pre-assembly (Yearbook 2014. Offshoreenergy.dk). Where right now the focus is only on pre-mounting turbine towers and/or Rotor Nacelle Assemblies (RNA), floating substructures open up the possibility to pre-assemble all substructure and topside components in the harbour, thus reducing the risk of brief weather windows and consequent waste of expensive resources. Independent procedures enable the preparation of the grid connection and of the sea bed anchoring system parallel to the assembly of substructure and turbine. The subsequent tow out and hook up can be done by standard tugs in much harsher conditions than current installation vessels can handle (H_{m0} max < 2m). That means larger weather windows

can be used, avoiding use and downtimes of specialised installation vessels, some having day rates of approx. 200.000€, compared to day rates of standard tugs in the range of 10.000€.

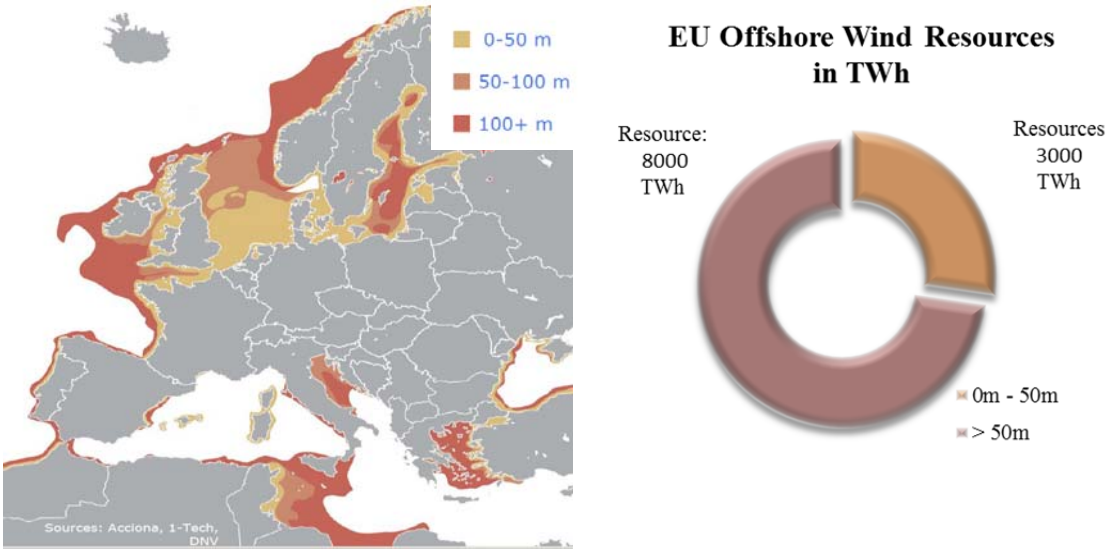

Figure 1: Offshore wind energy resources (right picture) as a function of water depth (left figure) in Europe. Resources according to EEA wind report 2009 (shallow water wind resource) & ORECCA project 2011 (deep water wind resource).

5. FLOATER & MOORING CONCEPTS

For offshore applications the main floater concepts can be divided into either mooring stabilized or ballast stabilized. Mooring stabilized structures are almost exclusively called tension leg platforms (TLP), which rely on excess buoyancy counteracted by vertical tensioned mooring lines. The basic principle is a floating body whose buoyancy exceeds significantly the light ship weight plus dead weight. Stability is obtained through restraint by a tension anchoring system. The advantages are relatively small structural dimensions, small footprints and small rotational motions. However, the small dimensions lead to the fact that TLP FOWTs are not self-stable. In essence that means that their in-place stability relies on the mooring system. Ballast stabilized structures however are self-stable and the mooring system has mainly a station keeping role. Such structures can be divided into either spar type structures or semisubmersible structures. Both systems require larger structural dimensions. The spar type structure has a large vertical extent; semisubmersibles have normally a large lateral extent. In addition, mooring systems are of catenary type, which consequently lead to large footprints (see Figure 2).

Generally speaking, station keeping systems can be divided into five groups and a brief overview of possible systems is given for the sake of completeness:

- High Vertical Load Plate Anchors are suitable for sand, silt and clay. They are normally driven or sucked to target depth, the guidance system is retrieved and the initially vertical plates are rotated into horizontal position to secure maximum capacity.
- Pipe-Pile anchors, for sandy or clayey sea beds have so far been the standard solution for TLP installations, where cylinders are simply driven or sucked into the sea bed and resist the applied loads by vertical friction.
- Drilled-Grouted anchors are most suitable for sea beds consisting of rock. In such a case the drill can either be retrieved and anchor components are grouted within the drill hole, or the drill itself is designed to remain in place and serves as mooring attachment point.
- Deadweight anchors are placed on the sea bed and have large self-weight, usually achieved by concrete. The suitability on inclined sea beds is poor, and they should only be considered for very hard soil conditions. To achieve high holding capacity, expensive heavy lift vessels are required for installation.

- Drag embedded anchors are dragged into the sea bed and can be applied in clayey as well as sandy conditions. Usual embedment depths are around 20m w.r.t. mudline. A disadvantage is that the loading direction should be nearly horizontal and the holding capacity becomes critical if the line angle at mudline becomes too large, which consequently requires large footprints.

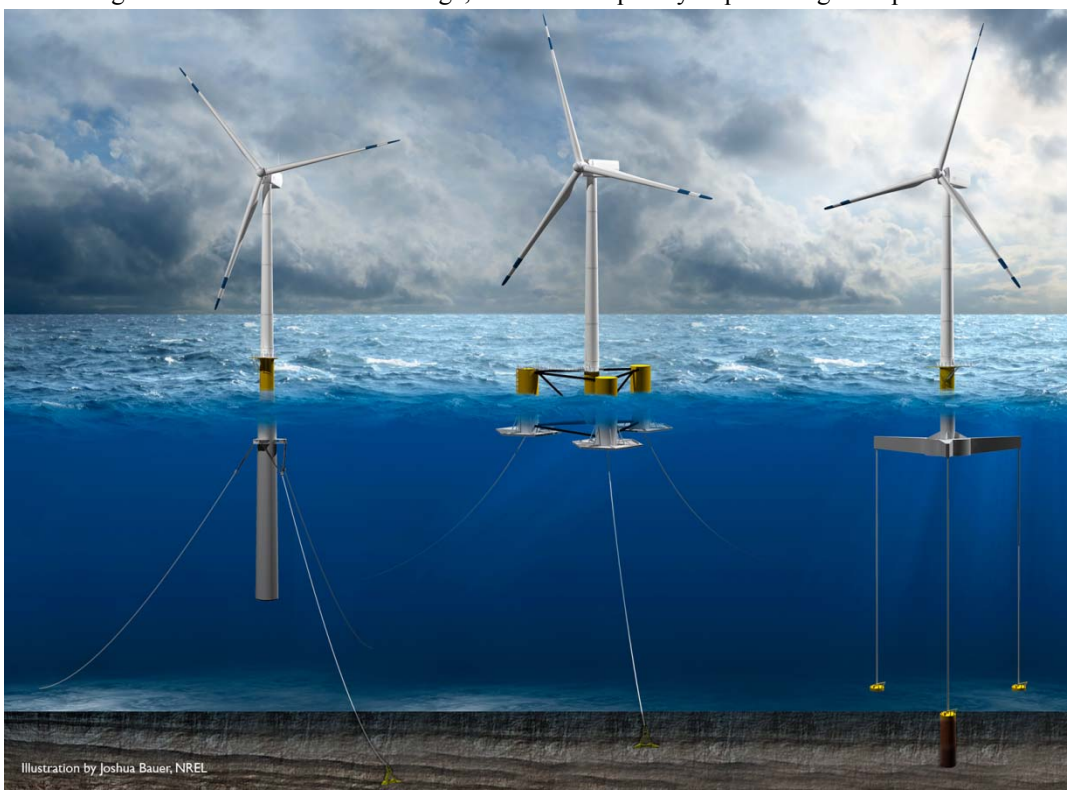

Figure 2: From left to right: Spar type FOWT, Semisubmersible type FOWT, TLP type FOWT, (Joshua Bauer, NREL).

The most common anchor systems used in FOWT station keeping systems today are catenary lines with drag anchors, due to the fact that drag anchors are very common in the offshore industry, i.e. off the shelf product, easy to install and proof. The catenary lines are usually chains with studded links. The stud increases the weight and provides stability in the lengthwise direction of the chain link. An example of the described layout is given in Figure 3.

Figure 3: Drag Anchor with studded chain. Source: http://www.vryhof.com.

6. STATE OF FOWT TECHNOLOGY

Several research calls, governmental acceleration programs and prototype initiatives document the increased momentum to lead the design of FOWT to an industrialized level. However, the price/performance ratio is still on a prototype stage, which implies an order of magnitude more expensive than established technologies. Numerous academic FOWT design can be found, but will not be further reviewed here, due to the industrial focus of the current work. An exception however is one academic project that finally led to an industrial scale design and might be seen as a good "How-To" example. The project is described in Utsunomiya, (2013), and is the forerunner of the Toda Corporation Spar, see Table 1. A 1/10 model of a hybrid spar, using precast concrete segments combined with a steel upper part is used to demonstrate the concept feasibility by performing sea trials. Good agreement was found for most of the motions comparing a simple in house code to the measured responses. Of interest for this study was not the actual layout of the test or of the structure but the general approach, i.e. doing sea trials with a scale model. Considering the wave energy test centre at Hanstholm, Denmark, and the infrastructure associated with it, pursuing the initiation of something similar is likely to be worthwhile. The biggest turbine vendors are located in Denmark and the relationships with industrial and university partners are close. The site at Hanstholm, would be well suited to carry out sea trials with a 1/2 or 1/3 scale model of a shallow water FOWT, i.e. around 50-60 meters in 1/1 scale.

Globally there are more than 30 FOWT projects in different development stages; however the developments concentrate on US, Japanese and European Waters. An extensive overview of industrial scale projects is given by Bossler (2011). Following the tradition of being the forerunner in offshore wind, several projects in Europe have been initiated; the most advanced will be summarized.

In two different research projects (Ocean Lider and Flottek), Spanish Iberdrola develops two concrete FOWT TLPs, where a 2MW and a 5MW turbine are intended to be used. Additionally Iberdrola has invested in the Maine (US) based Aqua Ventus floating project supporting the research. On the 8th of July 2014 the European commission awarded €33.5m to the Spanish Balea Wind power project that intends to install two 5MW and two 8MW turbines on either TLP or semisubmersible floaters in the Bay of Biscay. Another €34m have been granted to the Spanish FloCan5 project consisting of five 5MW turbines on concrete semisubmersibles off the coast of the Gran Canary island. In the framework of the EU-project FLOATGEN, France-based IDEOL intends to install a 2MW Gamesa turbine on the substructure in 2015. Their floater comprises a concrete ring shaped hull, which by entrapping water, adds additional damping to the system. Within the same framework, in 2015 Acciona will also erect a 3MW turbine on top of a floating substructure, designed by Olav Olsen, an as yet rather unknown designer in the offshore wind industry. Information about the type of the floater are not yet available. Blue H, Netherlands, has two TLP structure prototypes off the coast of Italy. The company is currently aiming at a demonstrator by 2015, conditioned on partners that support the finance and construction. The German GICON plans the installation of a prototype during 2014, after successful tank testing their TLP system at the HSVA (Hamburger Schiffsversuchsanstalt) and at MARIN in the Wageningen, Netherlands. Technip is leading the VERTIWIND and the InFlow demo projects. Both focus on the industrialisation of vertical axis FOWT. In the framework of the first project a 2MW prototype is supposed to be installed, whereas the second project serves as the basis for a 13 unit wind farm off the French south coast. The project is delayed due to authorisation issues, but the installation of the first turbine is aimed to be mid-2015.

Besides the described research projects five industrial scale plants FOWT are in operation, summarized in Table 1.

Table 1: Overview of industrial scale FOWTs in operation

No.	In operation since	Name	Turbine	Floater type	Country
1	2009	Statoil Hydro	Siemens 2.3MW	Spar	Norway
2	2011	Principle Power Windfloat	Vestas 2MW	Semisubmersible	Portugal
3	2013	Toda Corporation	Hitachi 2MW	Spar	Japan

4	2013	Mitsui	Hitachi 2MW	Semisubmersible	Japan
5	2013	Japan Marine United	Hitachi 66kV Substation	FOSS Offshore Substation	Japan

Looking at Table 1 it becomes evident that Japan has taken over the lead in installed FOWT capacity. The Fukushima Floating Pilot Project accommodates the world's first floating offshore substation (FOSS) and two already installed 2MW FOWT. A strong industrial joint venture, consisting of Marubeni (project integrator), the University of Tokyo (technical advisor), Mitsubishi, Mitsubishi Heavy Industries, Japan Marine United, Mitsui Engineering & Shipbuilding, Nippon Steel & Sumitomo Metal Corporation, Hitachi, Furukawa Electric, Shimizu, and Mizuho Information & Research are realising this fast track project, which started in March 2012. It is planned to be extended with two Mitsubishi turbines, most probably the 7MW Sea Angel, on two semisubmersibles, where one of the sub structures has already been completed. The first turbine is scheduled to be mounted on the floater in December 2014. This would make the latter the most powerful FOWT in the world, having a hub height of 105m and a rotor diameter of 167m, see Figure 4. The draft is given as 17m and the rotor tip to be 185m w.r.t. still water level. The length of one side will be approximately 106m. Mitsubishi plans to exploit the already mentioned pre-assembly options that FOWT offer. The turbine will be mounted onto the floater at the quay side in Onahama port, thereby minimizing weather dependencies. According to the Mitsubishi Press Release (June 2014) chains, anchors and subsea cables have already been installed, meaning the site installation of the turbine is an independent operation.

Figure 4: Illustration of Mitsubishi turbine on a semisubmersible. Source: Mitsubishi.

In European waters two industrial scale prototypes are currently being operated: The spar type floater Hywind of the coast of Norway and the semisubmersible type Windfloat of the coast of Portugal. Both prototypes intend to make use of the recently established nursing market in Scotland. In April 2013 the Scottish Government revealed a £15m deep water development initiative, with increased support grants for FOWT (75% higher than the support for traditional bottom fixed structures). Such a protected financial environment is crucial in order to gain best practice experience and push the technological readiness level to the next stage. The Hywind pilot park project is located at the Buchan Deep Demonstration Site 25km off the coast, where 5 FOWT with a capacity of 30MW are to be installed in water depths from 95m to 120m, with three-point spread catenary mooring system extending between 600m to 1200m around the foundations. The draft will be around 70m to 85m. Compared to the Norwegian prototype, having a draft of more than 100 meter the targeted technological readiness level increase becomes obvious. The substructure contract for a Front End Engineering Design (FEED) and subsequent Engineering & Management Assistance has just been awarded to a Norwegian consortium consisting of Norwegian Geotechnical Institute (NGI), Dr.techn.Olav Olsen AS and Principa North AS under the lead of Aibel AS.

The next stage of a Windfloat realisation, the Kincardine Offshore Wind Farm, is located 13km of the coast, close to Aberdeen. 8 FOWTs are to be installed in 60m to 80m water depth. The project is however not as progressed as the Hywind pilot park. The UKs' Crown Estate wants to develop a demonstrator, targeting a commercially viable solution by 2020. Funding has been granted to Glosten Associates, who have been contracted to carry out a front end engineering study using their TLP design. The intention is to deploy a FOWT structure carrying a 6MW turbine in 2015 off the coast of Cornwall in 60m water depth and design significant sea states of 10m. An artist's impression can be seen in Figure 5.

Figure 5: Artist impression of three legged TLP structure "PelaStar". Source: Glosten Solutions, Inc., Seattle, Washington.

Besides national governmental initiatives, European research support is also an essential bridging mechanism to further mature complex technological systems like FOWTs. The Horizon2020 call (H2020-LCE-2014-1) of the EU states explicitly that new innovative substructure concepts, including floating platforms are needed for water depth beyond 50m, in order to push the development of competitive low carbon energy generation. It is the intention to reduce the overall reduced project risks as well as life-cycle costs. Previous or currently running international research projects, such as Innwind, OC5 or FLOATGEN had so far not the focus on extreme and failure cases. However in exposed waters these can be the crucial cases that increase the risk of intensive maintenance cost or even require the replacement of components for a whole wind farm. It seems

reasonable that the subsequent production loss together with the repair costs thereby leads to a dramatic instantaneous increase of Cost of Energy (CoE).

7. INVESTIGATED FOWT

The FOWT modelled in the current work is a TLP structure based on a conceptual close-to-industry design, kindly provided by Glosten Associates, see also Figure 5. The mass is approximately 40% of the buoyancy and the topside mass is approximately 40% of the foundation. The total mass including the turbine is approximately 2000t. The radius at the surface is less than 10m and the radius of the outermost point is 35m and the draft is approximately 25m. Due to non-disclosure agreements, the actual dimensions cannot be made public. For the same reason, the initial turbine was replaced by the well-known NREL 5MW turbine, (Jonkman et al, 2009) and consisted of a tower and a RNA representation. Figure 6, shows the numerical model in ANSYS AQWA (2013) and two physical model layouts.

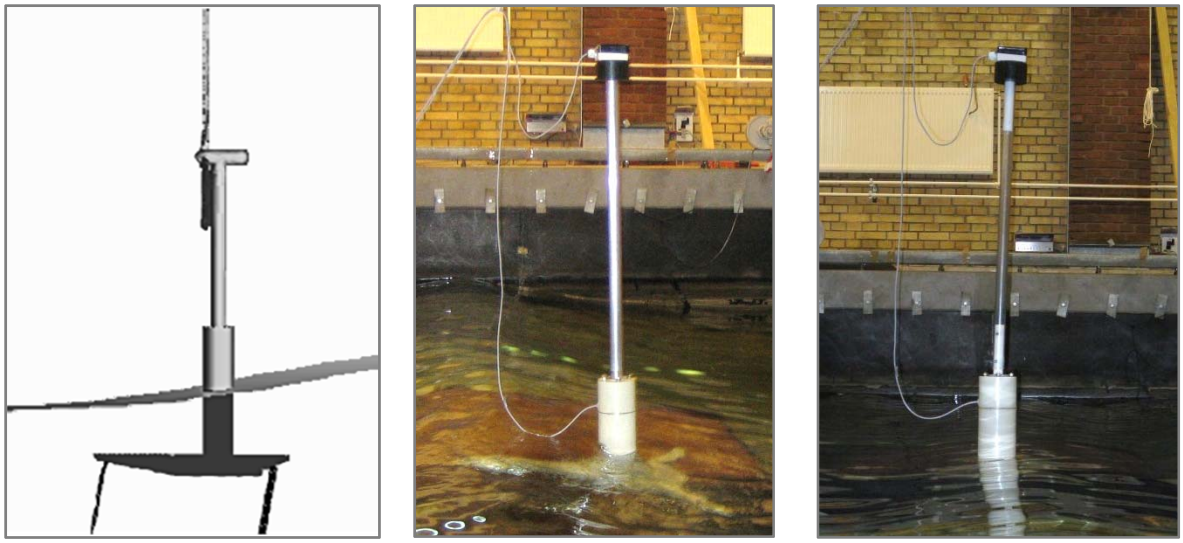

Figure 6: Left: Numerical representation of the TLP FOWT. Centre: physical model in regular waves with topside including stiff tower and lumped mass RNA representation. Right: Physical model in regular waves with topside including flexible tower and lumped mass RNA representation.

8. CHALLENGES IN FOWT DESIGN

An essential part of the author's work was the physical model testing and the subsequent validation of a numerical model development. A brief review on latest academic model test campaigns and on their related code validations for TLP and semisubmersible FOWT is given. Model tests and/or respective numerical comparisons on spar-type FOWT are discarded in the following review, due to their very limited applicability for intermediate or even shallow water. Hence the results of the current work would not be relevant for that substructure type.

Although the current work assumes that the gyroscopic effects caused by the rotor, as well as the elasticity of the blades are of secondary importance in ULS conditions, it is important to highlight a general challenge in FOWT model testing. That is the mismatch between Reynolds number and Froude number scaled models, which is inherent especially in operational FOWT scale models. It is common standard to conduct physical model tests, such that the prototype and the model have the same Froude number. However, this yields to rather low Reynolds numbers, which in return influences the lift and drag coefficients. Particular for wind turbine blades this has a significant impact, as it results in too low thrust coefficients. In order to reproduce the Froude scaled aerodynamic forces, one would need to increase the wind speed significantly. Consequently, would the drag on the whole system increase and therefore disturb the signal. Fowler et al. (2013) presented an approach, how to modify the blade layout, i.e. the profile of the blades. Key Froude scaled parameters, such as length and rotor operational speed are kept and in parallel the Froude scaled Reynolds number thrust matched the numerically predicted thrust. That improved the performance of the physical turbine model significantly, when compared to the geometrically scaled blades.

There are significantly fewer physical model tests on spar, semisubmersible or TLP FOWTs, than for Oil and Gas floating structures. Representatives of all three floater concepts have been tested by the DeepCwind consortium. Goupee et al. (2012) compared their performance by assessing the measurements. The investigated TLP showed the lowest spectral response of the nacelle acceleration and tower base bending moment in the low frequency range, i.e. wind excitation, and medium frequency range, i.e. linear wave excitation (operational conditions). The Semisubmersible and spar type floaters, showed larger responses, due to their very low natural pitch frequencies. However, the TLP showed a significant excitation at its high natural pitch frequency, where the excitation originated from the 2nd order wave sum frequencies. The response energy was even higher than the first order response energy. In an extreme sea state, the response energy for all three structures was concentrated around the linear wave excitation range. The spectral mooring responses showed an order of magnitude larger energy content for the TLP system than for the other two systems. It is interesting to note that the 1P frequency is clearly depicted, which was assumed to be caused by the vertically stiff TLP system. A subsequent paper from Kimball et al. (2012), identified areas of improvement by comparing the DeepCwind experiments against some numerical studies, carried out with the time domain code FAST from NREL, (Jonkman and Buhl, 2005). The respective focus was put on the semisubmersible representation. Even though the linear wave response matched well, the 2nd order difference frequency was grossly underestimated, especially for the surge response. Secondly it was found, that the tension on the catenary mooring layout was as well underestimated, which was assumed to be due to a combination of the missing higher order response and a quasi-static mooring model. The findings above triggered a further development of FAST, which will be briefly described in section 9.

The experiments and numerical model validation on a FOWT presented from Philipe et al. (2013), was carried out for a three column semisubmersible FOWT including heave plates. A Froude scaled model was equipped with an operational model of the NREL 5MW research turbine, which was able to reproduce the scaled thrust force. In general, a good agreement was found between both models. The interesting part of the numerical model, which distinguishes it from other code developments, was the inclusion of the non-linear Froude Krylov force together with the Morison contributions for braces and heave plates, linear hydrodynamic added mass, radiation damping and diffraction loads. Even though not incorporated in the current work, the inclusion of the non-linear Froude Krylov is recommended as a future development.

Towards the results of the TLP physical model tests, carried out by the DeepCwind consortium, a numerical comparison was carried by Prowell et al. (2013) out using again FAST. The version of FAST used, did not allow considering second order hydrodynamics, nor did it allow using measured wave elevation. For some regular wave test, it was shown that the energy in the pitch response spectrum was lower predicted than actually measured. Subsequently the numerical model under-predicted the platform pitch acceleration. Considering that in physical applications all waves develop higher harmonics, it was assumed that such higher harmonics caused the differences. During irregular storm seas the number of observed slack line events was higher than predicted by the numerical model, in particular for a parked rotor. The fairlead, which experienced the slack lining, was actually the aft fairlead of the three armed TLP, i.e. the TLP faced into the waves with the opposite two arms. It was assumed that the wind drag on the parts above the water line was under predicted and hence an additional overturning moment contribution was missing. However, it is the author's opinion that, neglecting the correct viscous forces above still water level might also have been a cause. The power spectra of the tendon tension did not show a distinct peak for the surge natural frequency; however the pitch natural frequency, being an order of magnitude higher, was clearly visible.

During extensive numerical studies, Matha (2009) compared the response amplitude operators (RAO) of the time domain solution in FAST to the frequency domain results from WAMIT, Lee et al. (2006), for a FOWT TLP structure. A simplified representation of a TLP structure, i.e. a large main cylinder with slender spokes was exposed to linear irregular waves as hydrodynamic boundary condition, no comparisons to physical tests were carried out at that time. FAST used the hydrodynamic coefficients calculated by WAMIT and it additionally included the flexibility of the topside, i.e. of the wind turbine. It was the first time that a change in responses, for the pitch and roll RAOs and natural frequencies, was observed, and traced back to the flexibility of the topside. Bae et al. (2012) conducted a similar study and underlined the importance of the tower elasticity. In an irregular wave simulation without aerodynamic dampening (parked rotor) an almost 200% increase of the maximum pitch motion was observed for a flexible tower configuration compared to a rigid body approach. It was concluded that the tower design is an essential part in order to control the dynamics of FOWT TLPs. The work from Bachynski and Moan (2012) supported the above as well, by comparing a linear frequency analysis and a non-linear time domain analysis. For a wave-only analysis as well as for a coupled wind-wave analysis, the non-linear tool, which included the tower flexibility, clearly showed higher tower top accelerations. It was found that for large sea states this effect was more pronounced.

An extensive overview of currently applied FOWT analysis software packages and combinations of software packages can be found in the OC4 project (Offshore Code comparison collaboration continuation), Robertson et al. (2014). In the scope of the project 19 different codes have been compared, by assessing their predictions for a semisubmersible FOWT. The majority of the codes use a combination of multi-body or FE model for the topside, i.e. the tower and RNA, and a rigid body representation for the substructure, i.e. the floater. It appears that several packages use FAST, or modules from FAST, in order to represent the turbine behaviour accurately. The hydrodynamic loading was generated by potential flow, the Morison approach or by a combination of the two applying regular and irregular linear waves. Although very far progressed, the numerical tools are not yet matured and common industrial design procedures have not yet been established due the complexity of the system. The latter becomes evident when considering the characteristics that distinguish FOWT from former well established floating systems, e.g. Oil and Gas systems, as subsequently summarized.

a. Traditionally large volume floating structures have been considered rigid - the influence of their structural dynamics onto the global system behaviour was thought to be negligible. However the high flexibility of FOWT topsides including the RNA and tower, change the global system's response. Figure 7 is taken from Wehmeyer et al. (2014) and compares the influences of three different tower flexibilities onto the global pitch motion natural frequency. In order to validate a numerical model, termed the hybrid model, the results are compared against two measured responses: a flexible and a stiff tower layout, and additionally compared against a fully rigid body solution, (Wehmeyer et al., 2014). The results show a shift from 2.05Hz to 1.75Hz, i.e. a decrease in motion eigenfrequency for the fully rigid body pitch response to the flexible topside body pitch response respectively. In prototype dimensions, that means a shift of the pitch eigenfrequency from 0.229Hz to 0.196Hz and

thereby a shift towards more energetic wave frequencies. Additionally are both pitch eigenfrequencies, i.e. of the very stiff tower layout and of the flexible tower layout, outside of the allowable frequency range as of today, i.e. an excitation might occur due to one blade passing the turbine tower. Current bottom fixed structures, which only need to consider structural excitation, have soft-stiff substructures, i.e. their allowed structural eigenfrequency range is determined by the 1P and 3P (blade passing tower) frequencies of the turbine, e.g. ~ 0.25Hz – 0.33Hz. As the observed eigenfrequencies of the floater are below that, an excitation of the pitch motion would occur. It is however expected that future larger turbines will have a lower frequency range, with 5rpm to 10rpm. That would result in allowable frequency ranges from 0.17Hz – 0.3Hz and consequently would no resonance occur between the blade passage frequency and the eigenfrequency of the pitch motion. Generally, this adds therefore another layer of complexity, as not only the structural eigenfrequencies need to be considered during the substructure design, but also the global motion eigenfrequencies. In the present case, all pitch eigenfrequencies would be below the allowed design envelope. For the current work this subject is not of relevance as only ULS conditions are evaluated (parked turbine). For FLS conditions however, this would be a highly important aspect. It seems sensible that especially for the pitch motion, having a large impact on tower and interface flange fatigue, the global eigenfrequency should be outside of any excitation range given by the waves or by the turbine.

b. FOWT are prone to be composed of structural parts being excited by different wave force characteristics. Due to the very low payload, lightweight structures are possible, which usually results in small dimensions with slender structures at the free surface, but voluminous submerged parts. The submerged parts are prone to be excited by diffractive wave forces in large as well as in small sea states. In smaller sea states the surface piercing parts will be dominated by diffractive wave excitation as well. However, in large sea states the surface piercing parts will be excited by hydrodynamic viscous drag, and it seems sensible to consider these contributions up the free surface. As an example the currently assessed FOWT can be mentioned. The dominating wave excitation forces are evaluated according to the wave force regimes depicted in Figure 8 (Figure 9 indicates the associated structural parts as mentioned in the legend of Figure 8). The structural parts of the assessed TLP structure are assigned to their respective dominating wave excitation force from the average significant wave height (in prototype scale) of model test sea states and three respective maximum wave heights. The need for a hybrid solution becomes clear, considering all inertial wave excitation as well as viscous drag wave excitation. Such a hybrid approach is supported by suggestions in the recently published FOWT standard DNV-OS-J103 (2013).

c. Considering that the offshore wind industry intends to install dynamically sensitive and viscous hydrodynamic drag dependent floating structures at water depth, from 50m to 60m onwards, a first or second order wave theory approach may not be sufficient to describe realistic wave shapes. Therefore a higher order wave theory seems necessary. Figure 10 depicts the average significant wave height (in prototype scale) of model test sea states and three respective maximum wave heights. Assuming this to be a typical significant wave height for a water depth around 60 meters, it demonstrates that the H_{m0} value is on the edge of the 2^{nd} order theory validity. It might be justifiable to apply a 2^{nd} order sea state in such conditions; however common practice in the Offshore wind industry suggests higher order wave theories might be necessary for the design waves H_{max}. Figure 10 shows that waves higher than the significant wave height are better represented by 3^{rd} order Stokes or symmetric Stream-function waves.

From the above it can be concluded that the full complexity of the system - a very heavy lumped mass, supported by a slender pile, which in itself is located on a floating body that is excited by steep waves – needs to be considered in a design. The direct solution would be the application of CFD (Computational Fluid Dynamics), however, the current software and computer resources are still too expensive to be used on an industrial basis in FOWT design, which is why simpler engineering methods are required, considering the above outlined influencing factors.

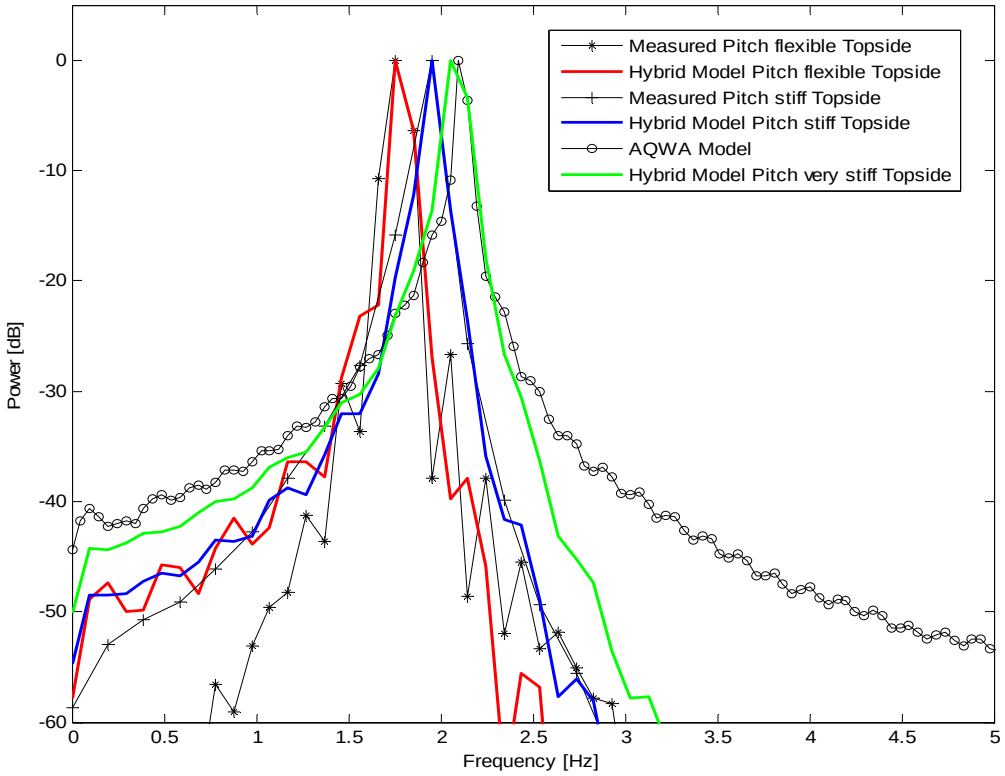

Figure 7: Change of system behaviour, by inclusion of flexible topside. Measured responses are compared to numerically obtained responses for three different topside flexibilities. (Wehmeyer et al., 2014)

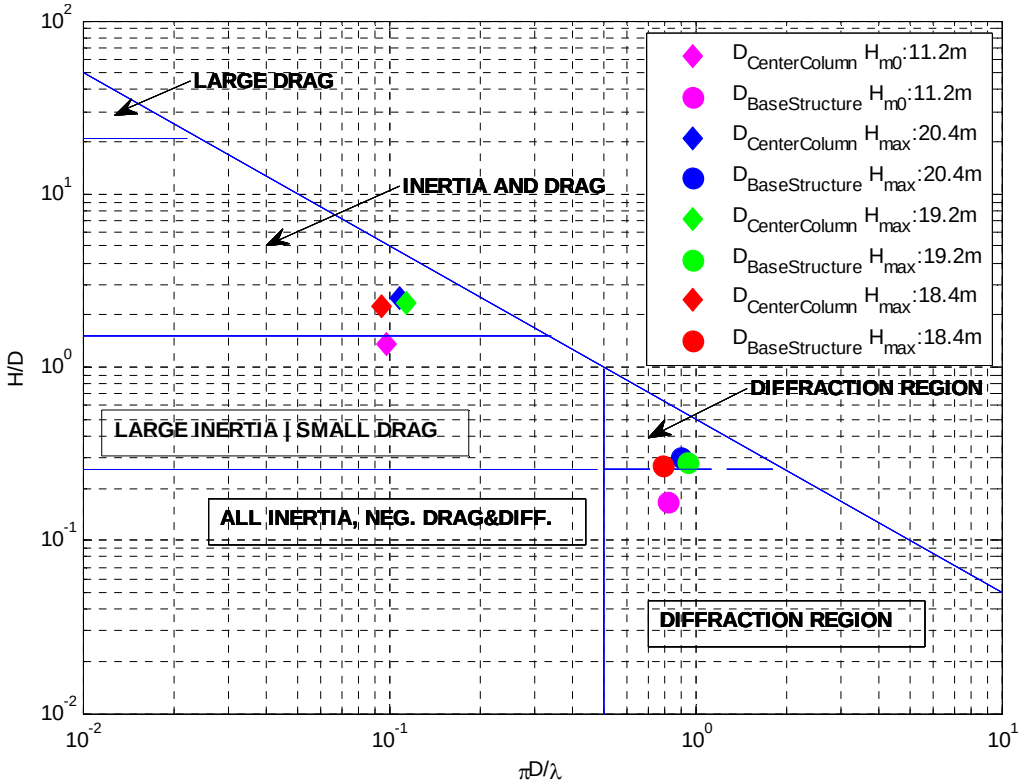

Figure 8: Dominating wave force regime for the main structural parts. The periods are the mean of the measured peak period values, (Wehmeyer et al., 2013)

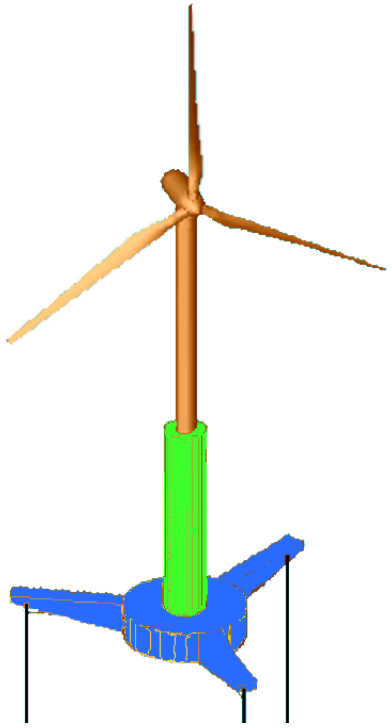

Figure 9: Main structural parts. Green shows the surface piercing centre column, blue shows the submerged base structure including the three tendons.

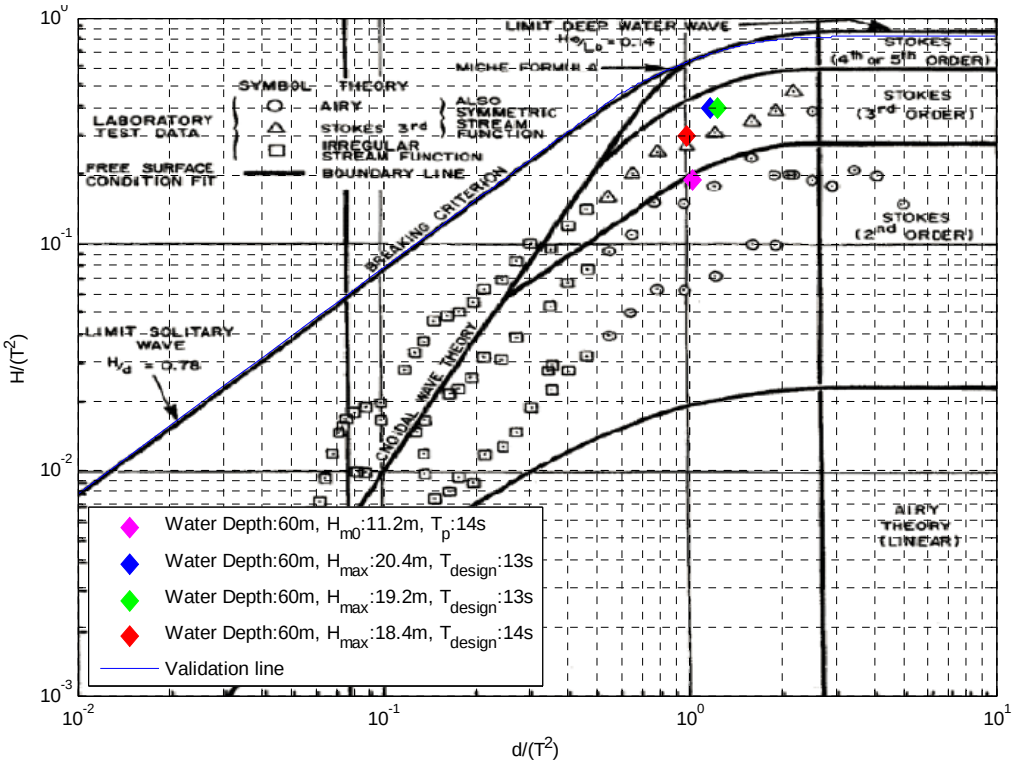

Figure 10: Validity ranges of wave theories and location of measured waves in prototype scale. The background picture is taken from Chakrabarti (1987).

9. STATE OF THE ART ULS ANALYSIS

The wind loads on the tower as well as the wind loads on the blades during fault are important in the design of offshore wind turbines and all industrial design applications account for them. However the hydrodynamic forces remain the predominant design driving loads, when the turbine is parked in ULS conditions. This study neglected therefore the wind loads, as the primary focus was a description/understanding of the hydrodynamic excitation and it seemed straight forward to add a wind load model in later stages for such conditions.

Analyses of offshore structures in ULS are performed to verify the maximum load-carrying resistance of the structure. Towards the background of Figure 10, it can be stated that the ULS analysis of any structure in intermediate to shallow waters requires a hydrodynamic excitation model, which considers the nonlinearities of the wave. DNV (2013) recommends two approaches for the case where waves become steep and non-linear:

A. 2nd order irregular waves
B. Embedding of a non-linear wave into an irregular Airy wave model

Until recently regular non-linear waves, mostly based on Stream-function theory, Fenton (1988), have been used in the industry for assessing large wave impact. Wehmeyer et al (2013) apply that method in order to compare measured pitch responses in non-linear regular waves to numerical simulations as an initial performance indicator.

Option B is well established and is the current industry practise on how to estimate the ULS loads from large non-linear waves impacting on bottom fixed offshore wind turbines. The challenge lies in the application of the same principles to FOWT, as indicated in Figure 11. Due to the possibilities, which are seen for further optimization of the ULS analysis for bottom fixed offshore wind turbines as well as for FOWT, the current engineering practise of ULS analysis will shortly be summarized and some recent developments will be presented.

The overall integrity of a structure is examined with design loads and design material properties. As mentioned, it is common industry practice to assess the structural responses in the ultimate limit states by exposing the offshore foundation to a linear sea state, where the highest linear wave is usually replaced by a Stream-function wave representation of the highest estimated maximum wave height, Figure 11 left and middle picture – at the point of highest wave impact. The latter is obtained assuming Rayleigh distributed wave, where subsequently the H_{max} can be estimated by 1.86 times the significant wave height, IEC (2009). The corresponding design periods should be in a range given by the well-known IEC equation, Eq. 1, IEC (2009), which relates the significant wave height H_S and the acceleration of gravity to the period that should be used for the design wave.

$$11.1\sqrt{\frac{H_S}{g}} \leq T_{Design} \leq 14.3\sqrt{\frac{H_S}{g}} \qquad \text{Eq. 1}$$

The hydrodynamic loading in terms of load per unit length F(t,x,y,z) for a given point in space (x,y,z) and time (t) is obtained by using Morison's equation, assuming slender structural parts, which do not change the incident wave. The drag and inertia coefficients are usually predicted as a function of the instantaneous Reynolds and Keulegan-Carpenter number. Waves are usually modelled using a JONSWAP-spectrum and the free surface elevation time series is generated by discretising the wave spectrum. The spectrum is discretised into a number of harmonic components with a constant frequency interval Δf. For each discrete frequency the corresponding harmonic wave amplitude is determined and each harmonic component is assigned a random phase. Typically, a time series with duration of 600 seconds is modelled with an additional initialization time of e.g. 50-200 seconds in order to ensure that any initial transients are damped out and therefore do not affect the dynamic responses. The wave kinematics for the irregular waves are calculated in accordance to linear wave theory in the time domain analysis. A site-specific maximum non-linear Stream-function design wave

replaces the maximum irregular wave in the time series by being "blended in". This allows for consideration of the dynamic behaviour of the structure introduced from the hydrodynamics during the design storm conditions. As the design storm conditions are covered, the simulation time is assumed sufficient.

OWT with Monopile foundation in non-linear wave

OWT with Jacket foundation in non-linear wave

FOWT in non-linear wave

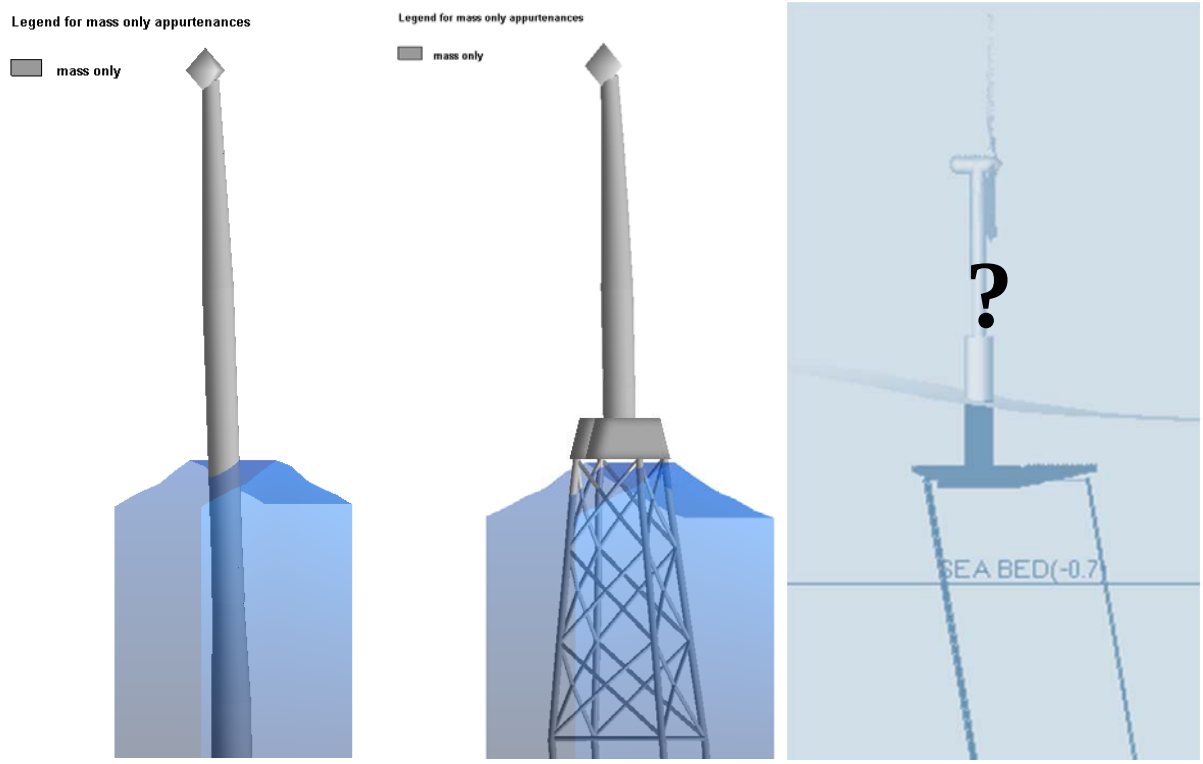

Figure 11: Left and Centre: Current state of the art numerical representation of non-linear wave impact on bottom fixed offshore wind turbine foundations; wave is generated using Stream-function theory. Right: Illustrating the challenge of numerical representation of non-linear wave impact on FOWT.

A very important, though not yet industrialised, step in wave load calculation on offshore foundations must be briefly mentioned and summarized here, as parts of it may be worth considering in future FOWT applications. The wave load project, Bredmose et al. (2013), recently presented a major development, i.e. a very detailed analytical approach for future wave loading analysis. In light of the increased momentum in XXL monopile development, the described method might be an alternative to the common best practice engineering approaches, as outlined previously. The report makes reference to the PhD thesis of Paulsen (2013), where the development and integration of a nonlinear potential flow solver and a CFD solver is extensively described. The time efficient integrated model showed an impressive fit to wave gauge measurements from physical model tests, and results produced can therefore be assumed very close to reality.

The project compared structural dynamic responses of a monopile structure in three different wave load realisations: Irregular linear wave loading calculated by Morison's type loading, irregular non-linear wave loading calculated by Morison's type loading and irregular non-linear wave loading calculated by a pressure distribution based on a CFD model. As input for all models a linear JONSWAP spectral model was used at the outermost boundary, after which the waves travelled along a mildly up sloping sea bed into the domain towards the structure. The irregular linear and the irregular non-linear wave realisations were obtained by the OceanWave3D solver (Engsig-Karup et al, 2009). The CFD loads were based on an integrated wave model, where the CFD solver was used for a smaller spatial domain close to the pile. The CFD domain's boundaries were defined using a fully nonlinear potential flow solver (OceanWave3D). The aero-elastic Flex5 model (Øye, 1996) was used to compute the responses of the monopile supporting a 5MW turbine. The potential flow

solver OceanWave3D is generally only accurate up to the point of breaking therefore loads from steep and near breaking waves may be overestimated (personal communication with Paulsen).

The difference between the linear irregular sea state and the non-linear irregular sea state was clearly shown by the obtained differences in fatigue damage. For large water depth (40m) it was found that the damage computed by the non-linear sea state was 18% higher. This effect however decreased with decreasing water depth, due to the wind loading dominating the fatigue damage and additionally due to the pile diameter, which decreased and consequently the wave load contributions decreased as well.

To identify the differences between the non-linear potential flow solver without the nested CFD domain and the non-linear potential flow solver with CFD solver, a ULS case was compared in which parked conditions were assumed in order to clarify the applied wave loading and consequent responses. The largest overturning moment at mudline was predicted by the OceanWave3D – Morison coupled loading, which was most probably due the ability of the CFD solver to simulate wave breaking and dissipation of energy. The OceanWave3D solver generated much steeper waves, which seem to induce more impulsive loadings. That leads to impulsive impacts which become very obvious in the overturning moment comparison at the tower bottom. Here the CFD calculations resulted in significantly smaller values.

The above outlined approach is without question the most accurate one in terms of load prediction on bottom fixed structures, which as such eliminate/minimize uncertainties in today's design. Therefore a thorough discussion on safety factors should however accompany the industrial implementation. However the disadvantage in terms of day-to-day bottom fixed offshore wind turbine engineering is that the bathymetry needs to be known in a spatial domain around the structure. If the bathymetry is additionally a function of time for a number of turbine locations, the challenge will be to firstly find an accurate bathymetry long term model and apply afterwards the fully non-linear (possibly with a nested CFD domain) approach. However, due to the larger water depth, the bathymetry at FOWT locations can be assumed much more stable than for example at near shore bottom fixed turbine locations. Therefore, the OceanWave3D solver might become an interesting alternative for sea state generation in deep water bottom fixed foundation analysis and FOWT analysis in the future. However, especially for large sea states the general water depths in which wind turbines are installed can still be termed intermediate or even shallow. Consequently will the waves interact with the seabed and change their shape and ultimately the associated kinematics. Generally speaking the resulting wave excitation loads can be divided into two contributions: inertia loads and drag loads. The simplest approximation for this is Morison's equation, (Morison et al., 1950), applicable for slender structures, which do not change the incident waves. Solving for the motion of a structure, a Morison type force can exemplarily be applied to solve an equation of motion, where no linear damping is assumed, Eq. 2.

$$M\ddot{x} + Kx = F_{Excitation} \quad \text{Eq. 2}$$

$$F_{Excitation} = \int_{SB} \left(\rho\pi \frac{D^2}{4} \frac{\partial u}{\partial t} + \rho\pi \frac{D^2}{4} C_a \left(\frac{\partial u}{\partial t} - \ddot{x} \right) + 0.5\rho D C_D (|u| - \dot{x})(u - \dot{x}) \right) dz \quad \text{Eq. 3}$$

$$(M + \rho V C_a)\ddot{x} = \rho V (1 + C_a) \frac{\partial u}{\partial t} + 0.5\rho A C_D (|u| - \dot{x})(u - \dot{x}) \quad \text{Eq. 4}$$

Where in a single degree of freedom system, M is the Mass and K is the stiffness. The excitation force, Eq. 3, is vertically integrated over horizontal sections of the wetted surface SB, where D is the diameter of the structure of the respective section, x is the displacement with which the body moves and u is the water particle velocity. Inserting Eq. 3 into Eq. 2 and assuming exemplarily a small body of mass in an oscillating flow with no hydrostatic stiffness, Eq. 4 is obtained, where V is the volume of the small body and A being the projected area of the small body perpendicular to the flow. The additional inertia term on the lhs is the added mass effect with C_a being the added mass coefficient, the first term on the rhs can be understood as the inertial part of the

excitation force (Froude Krylov and diffraction at the low frequency limit) and the second rhs term is the viscous drag effect, with C_D being the drag coefficient. However, floating structures are often characterised by being entirely or partially greater than 0.2 times the wave length, i.e. the floating body changes the incident wave. Therefore diffraction effects become important for such parts and the excitation forces need to be calculated as a function of wave frequency. Potential theory codes calculate the frequency dependent excitation force coefficients. The viscous force is neglected and only the inertial part of the force, consisting of the Froude Krylov and Diffraction force are covered by these coefficients. The 1st and 2nd order excitation force can be calculated as a function of wave elevation and phase. Even though the inertial 2nd order excitation forces have not been considered in this project, for the sake of completeness in relation to recent literature and for developments subsequent to the current project they will briefly be described.

For an irregular wave realisation the surface elevation is given by:

$$\eta(x,y,t) = \sum_{i=1}^{N} A_i \sin(k_i x - \omega_i t + \varphi_i) \qquad \text{Eq. 5}$$

Where A_i is the well-known amplitude of the sinusoidal regular wave realisation according to the spectral density. k_i is the wave number of the ith wave, ω_i is the wave frequency of the ith wave and φ_i is the random phase of the ith wave. Assuming long crested waves, the respective 1st order excitation force is given by

$$F_{exc}(t) = \sum_{i=1}^{N} A_i \Re\left(F_{exc}(\omega_i) e^{i(\varphi_i - \omega_i t)}\right) \qquad \text{Eq. 6}$$

$F_{exc}(\omega_i)$ is a complex number, where the phase is the phase shift of the excitation force with respect to the incident wave. $\Re$ indicates the real part, $F_{exc}(\omega_i)$ is the frequency dependent 1st order wave excitation coefficient and φ_i is the random phase chosen for the wave surface elevation realisation, being of importance for the correct excitation force calculation. The premise for the above application is that the exact amplitude and phase information are available, which compose the irregular sea state. For the application of recorded time series, e.g. from wave tank test the application becomes challenging. Alternatively, the first order excitation can then be applied by an Impulse Response Function representation (IRF), where the IRF is obtained by IFFT from the frequency domain coefficients. The excitation force considers at each time step a part of the future waves, which means that the excitation force vector F_i^{exc} is the results of the non-causal unit impulse response function h_i^{exc} per DOF being convoluted with the wave elevation η.

$$F_i^{exc}(t) = \int_{-\infty}^{\infty} h_i^{exc}(t-\tau)\,\eta(\tau)\,d\tau \qquad \text{Eq. 7}$$

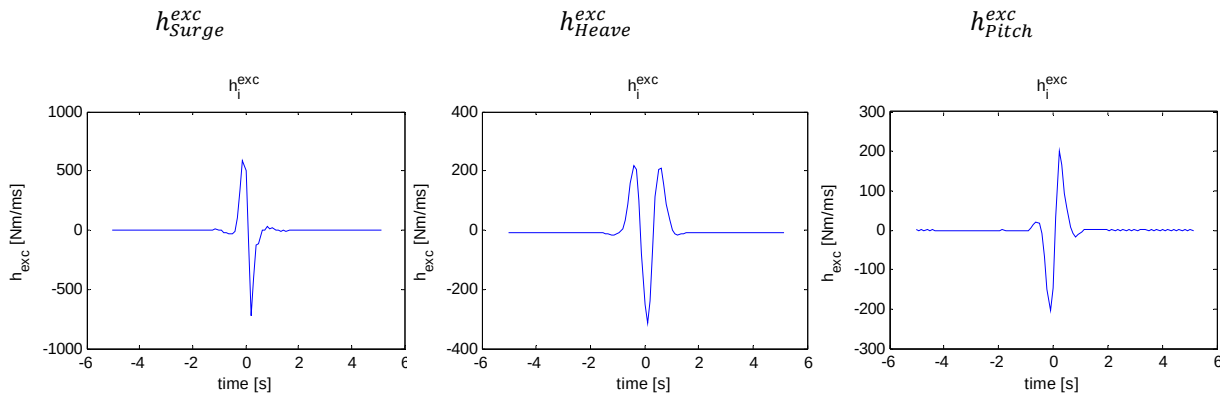

Figure 12: Excitation force unit impulse response functions for surge, heave and pitch.

Figure 12 shows the three h_i^{exc} functions, which are applied in the current work. However, in order to obtain accurate numerical responses, the waves need to be measured adjacent to the structure, i.e. in a line parallel to

the wave maker paddles, and the structure should only oscillate with small motion amplitudes. The first premise was not realised in the current project, as the wave gauges were applied in front of the structure, which is why the measured surface elevation could not be applied. A shift to the location of the floater, using linear theory, was assumed not valid due to the non-linearity of the waves.

The 2nd order excitation forces, i.e. due to the wave sum frequency and wave difference frequency contributions, are given equivalently. However, where the 1st order coefficients describe the relationship between the individual unit amplitude wave and the force exerted on the structure, 2nd order excitation coefficients are a function of the product of two wave amplitudes and have frequencies equal to the sum or the difference of the respective two wave frequencies, which is why they are called quadratic transfer functions (QTF). A thorough description of the second order inertial fluid forces can be found in Ogilvie (1983) or Journeé and Massie (2001). Assuming long crested waves, the respective 2nd order excitation is given as follows:

$$F_{exc}^{Sum}(t) = \sum_{i=1}^{N}\sum_{j=1}^{N} \Re\left(F_{exc}^{Sum}(\omega_i,\omega_j)A_iA_j e^{i\left((\varphi_i+\varphi_j)-(\omega_i+\omega_i)t\right)}\right) \quad \text{Eq. 8}$$

$$F_{exc}^{Diff}(t) = \sum_{i=1}^{N}\sum_{j=1}^{N} \Re\left(F_{exc}^{Diff}(\omega_i,\omega_j)A_iA_j e^{i\left((\varphi_i-\varphi_j)-(\omega_i-\omega_i)t\right)}\right) \quad \text{Eq. 9}$$

Where $F_{exc}^{Sum}(\omega_i,\omega_j)$ and $F_{exc}^{Diff}(\omega_i,\omega_j)$ are the complex frequency dependent 2nd order wave excitation coefficients, with frequencies equal to the sum and difference frequency of the incident waves respectively; and φ_i& φ_j are now the random phases of the interacting wave surface elevation being of importance for the correct excitation force calculation.

Similar to the first order wave excitation, it is possible to apply the second order wave excitation by a quadratic impulse response function representation, as discussed for example in Næss (2013). In this case the frequency domain based quadratic transfer function matrix (QTF) needs to be converted by a two dimensional IFFT into the non-causal quadratic impulse response function, which consequently is applied to the surface elevation by two dimensional convolution. This approach was not continued in the current project, though it can be stated that the inclusion of the higher order inertial loadings should be considered in subsequent developments.

However, $F_{exc}^{Sum}(\omega_i,\omega_j)$ and $F_{exc}^{Diff}(\omega_i,\omega_j)$ depend on the first order body motions. If the body motions are based on a natural frequency that does not consider the flexible topside, the direct application imposes a challenge for FOWT. A very recent communication with Jonkman (personal communication, 2014) confirmed that, however so far no studies have been conducted to quantify the deviation. Especially FOWTs that have high natural frequencies of their global rotational motions, i.e. where the topsides rotational inertia influences the first order global motions due to the flexibility of the topside, would experience an error in the second order loads. The challenge is that the fluid force exerted on the body is composed of a hydrostatic fluid force, a first order oscillatory fluid force and a second order fluid force. The second order fluid force consists, besides others, of a pressure term that is given by the integration of the pressure over the oscillatory pressure part on the wetted surface due to first order motions, i.e. the superposition of the first order wave height and the first order motion. If the second order frequency domain coefficients are determined by the first order motions that do not consider the influences of the flexible topside, the second order motions would be skewed. However, Jonkman (personal communication, 2014) stated that the influence of the tower bending flexibility on the pitch response was so far only found for TLP structures, not for semisubmersibles and spar type floaters. This is in agreement with the results in Bayati et al. (2014), where the pitch natural frequency peak of a time domain multi body computation is equal to the potential flow computation in the frequency domain. While this should still be validated by physical model tests, it appears logical that this effect is caused by the different natural frequencies ranges of the different floater concepts. Spar and semisubmersible floaters have normally very low natural pitch and surge frequencies (opposite to TLP structures), i.e. the influence of the RNA inertia on the tower bending is low due to low accelerations. Accordingly would the influence of the tower bending on the

global pitch motion be low. For the current state of the art, this has some practical implications, as the computation of first and second order force transfer functions can be assumed applicable for non-taut mooring structures.

A relevant observation concerning second order drift forces, was made by Pinkster and Huijsmans (1992), who investigated the low frequency responses of a vessel in shallow water. He showed by model tests as well as by computations that the oscillating part of the low frequency response becomes larger in shallow water, which is why this is assumed to be of relevance for FOWT. The effect can be explained by the stronger set down effect in the wave groups, being a second order wave-wave interaction effect.

Recently several efforts have been taken, to investigate the effect of higher order wave impact on floating offshore wind turbines. The work from Bachynski and Moan (2013), Bachynski (2014), Roald et al. (2013) and Bayati et al. (2014) focused on the additional inertia effects caused by the sum and difference frequency interaction of the wave.

Bachynski and Moan (2013) analysed four different single column TLPs with varying diameter and pontoon sizes (spoke at which end the tendon is attached) length in 150m water depth. The surface piercing diameters varied between 18m and 6.5m, and the displacement varied between 11866m^3 and 2320m^3 respectively. The hydrodynamic loads were computed by three different models, i.e. 1st order potential flow and linear viscous drag, first and second order potential flow and linear wave viscous drag and Morison's formulation. The linear wave kinematics calculated at still water level were applied to the free surface and all hydrodynamic loads were applied at the initial position of the structure, ensuring a correct phasing of the different forces. For the smallest diameter structure the Morison model showed good agreement to the potential flow results, however for the large volume structures a greater pitch excitation was found using the Morison loading model, particularly in severe conditions.

In Bachynski (2014), it was found that second order forces had an increasing impact on the fatigue damage in wind-wave misalignment situations. Interestingly in misaligned conditions the total fatigue damage was found to be generally smaller than in aligned conditions. This is actually not in agreement with current industry experience, considering that the aerodynamic dampening on the structures motion in highly misaligned situations is rather low. It seems that the damage was spread differently over the cross-sections and hence reduced the effect (personal communication with E.E. Bachynski). While not covered in this context, this subject is of high importance and should be investigated further. It was also found that the sizes of the submerged part (pontoons) had a considerable effect on the heave QTFs and consequently on the sum frequency of the heave motion. The structure with the higher volume pontoon resulted in the larger heave QTF.

Roald et al. (2013) discussed the effect of including the second order potential flow hydrodynamics and their effect on a spar type FOWT and a TLP type FOWT. It was shown that for the spar type structure the heave motion was significantly influenced by the difference frequency excitation. More importantly however, it was found that for the surge motion the aerodynamic excitation dominated the low frequency response and that the low frequency wave excitation force was almost negligible. For the TLP structure a significant influence of the motion responses was seen, where the second order effects even dominated the total responses. The TLP structure used was of large diameter, which supports the use of potential flow excitation. The assessment was done in the frequency domain, which did not allow for any non-linear contributions, e.g. hydrodynamic damping. As also pointed out, the challenge here is that the first order hydrodynamic coefficients can solely be obtained from the structures geometry, i.e. the first order wave forces are derived based on the assumption of a stationary floating body, however the second order wave forces are derived based on the assumption that the body is allowed to move responding to the first order wave forces. This implies however that the first order body motions are needed for the computation of the second order fluid forces. Especially for an FOWT TLP however, the rigid body assumption considered in the potential flow theory does not hold, which in essence means that potential flow computation of the correct second order fluid force is a challenge. Additionally, these forces have inertial character. The surface piercing part of other FOWT substructures however is often slender, which means that viscous effects correct to the surface elevation are of importance.

Bayati et al. (2014) discussed the effects of higher order hydrodynamics on a semisubmersible FOWT structure. The 1st order loads and responses were compared to the 2nd order loads by using the potential theory

solver WAMIT and subsequently compared to the responses from 1st order wave plus aerodynamic excitation and wave only excitation computed by FAST. Instead of using Newman's approximation, i.e. where the full difference frequency matrix is approximated by the diagonal term, the full second order load matrices as computed in the WAMIT were applied. For the investigated structure the surge, pitch and heave natural frequencies were below the wave spectrum, which is common for semisubmersibles. Consequently it was found that the difference frequencies in particular had a non-negligible impact on the responses. The first order wave-only surge responses computed by FAST and WAMIT matched very satisfactory. As one might expect a difference could be observed between the first order wave only excitation and the first order wave plus wind excitation, i.e. the surge motion showed a distinct low frequency peak due to the wind, with non-zero energy, i.e. the mean wind speed at zero frequency. Especially for the largest sea state, i.e. H_{m0} = 7m, the second order difference frequency excitation resulted in a spectral peak of the same order of magnitude as the wind excitation at the surge natural frequency. Consequently, that confirmed the importance of the inclusion of second order hydrodynamics and triggered further development of the FAST code, Duarte et al. (2014).
Another way of including non-linear inertial effects is to account for the instantaneous Froude-Krylov force. Linear potential flow assumes the incident wave force, caused by the Froude-Krylov force (the undisturbed pressure distribution on the structure), and a correction due to the diffraction of the wave (disturbance of the wave due to the structure), to be calculated on the mean wetted surface. A nonlinear approach would be to estimate the Froude-Krylov force on the instantaneous wetted surface assuming that the Froude-Krylov force is the main component of the respective hydrodynamic force, Babarit and Laporte-Weywada (2009) as well as Philipe et al. (2013). However, this was not accounted for in the current stage of the development.

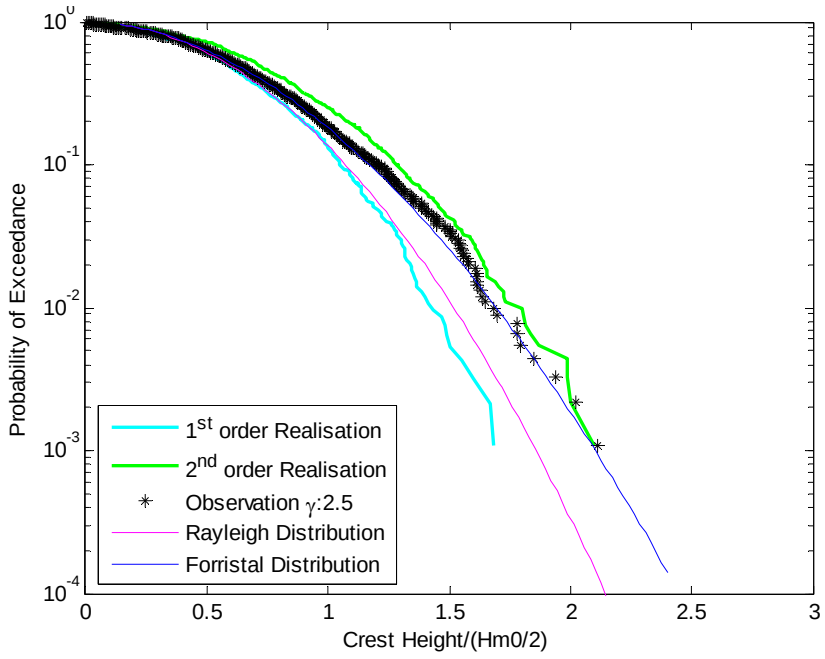

Figure 13: Normalised Wave Crest distribution from observation, 1st and 2nd order irregular sea state realisations and respective distribution models. (Wehmeyer and Rasmussen, 2014).

So far, the above concerned the inertial part of the wave excitation. Considering however, that FOWTs usually have rather small water plane areas with slender surface piercing dimensions, viscous effects can be assumed important. The viscous hydrodynamic drag force is a function of the relative velocity between the floating structure and the wave particle velocities per projected area section of the structure. A steeper, more non-linear wave will therefore produce a higher drag force than a sinusoidal wave and the steeper the wave is, the higher the drag force will be. It was shown by Forristall (2000) that even in deeper waters a higher order wave elevation time series is better suited to resemble the natural sea surface in storm conditions than a 1st order realisation of the sea state. This is also supported by Figure 13 (cf. Paper in Appendix 4), where a wave crest

time series from tank test is compared to first order realisations and second order wave crest realisations and as well against the respective distribution models. For more information on the derivation of the second order wave realisation see Appendix 4. A higher order (in this case 2nd order) sea state model yields a wave shape with shallower troughs and higher crests and a recent application can be found in Agarwal and Manuel (2010). They assessed the impact of second order hydrodynamic effects on a bottom fixed structure and showed unsurprisingly that the second order model delivered higher loads than a first order load. Morison's approach was applied to determine the wave excitation force on a 6 meter monopile in 20 meter water depth supporting a 5MW reference turbine. An increase of 2% and 18% of the ten minute maximum for the overturning moment at mud line was found from H_{m0} = 5.5 and H_{m0} = 7.5m, respectively. On the basis of the provided information, it can be assumed that the maximum fore-aft tower bending moment is due to the viscous drag, as the peaks occur simultaneously to the wave crest peaks. Assuming that the applied second order irregular wave model delivers more realistic crest height distributions especially for large sea states, the importance of the viscous contribution above the still water level is highlighted.

In line with Figure 8, it is therefore assumed that the viscous force contributions, being a function of accurate wave elevation and kinematics, see again Figure 13, are an important part of the incident wave excitation for the surface piercing part of the investigated FOWT. Hence combines the numerical model, which is developed in the current project, linear radiation and diffraction effects and considers additional non-linear terms, i.e. the hydrodynamic viscous drag originating from non-linear wave descriptions.

10. RESEARCH WORK

The author's work assesses the two proposed methods, namely option A and B (2nd order irregular waves and embedded non-linear wave into an irregular linear wave) as described in section 9, for a FOWT TLP and compares the results to observations from physical model test data. The current work however modifies option B and embeds a Stream-function wave into a 2nd order non-linear irregular wave, as the non-linear incident wave model resembles the background surface elevation better (and probably also the wave kinematics), (Wehmeyer and Rasmussen, 2014). A key-performance-parameter, i.e. the loading of the bow tendon, is representatively assessed in a ULS case.

In order to reach this point the project first needs to define the ULS environmental parameters, i.e. an environmental design basis is developed (work package 1). Secondly a physical model test layout is required (work package 2). Thereafter, a numerical model is developed. It is deemed feasible to first verify the model against measured pitch responses in regular waves and subsequently carry out a final key-performance-parameter evaluation (work package 3 and 4). Each work package resulted in a paper. Following the described work packages, the four respective abstracts and conclusions will be cited in four subsequent sections. Each of the four work packages is complemented by more detailed information on the work carried out.

10.1 Generic Hurricane Extreme Seas State. An engineering approach (Wehmeyer et al., 2012, Conference Paper)

Abstract: *"Extreme sea states, which the IEC 61400-3 (2008) standard requires for the ultimate limit state (ULS) analysis of offshore wind turbines are derived to establish the design basis for the conceptual layout of deep water floating offshore wind turbine foundations in hurricane affected areas. Especially in the initial phase of floating foundation concept development, site specific metocean data are usually not available. As the areas of interest are furthermore not covered by any design standard, in terms of design sea states, generic and in engineering terms applicable environmental background data is required for a type specific conceptual design. ULS conditions for different return periods are developed, which can subsequently be applied in site-independent analysis and conceptual design. Recordings provided by National Oceanic and Atmospheric Administration (NOAA), of hurricanes along the US east coast and the Gulf of Mexico (1851 - 2009) and Japanese east coast (1951 -2009) form the basis for Weibull extreme value analyses to determine return period respective maximum wind speeds. Unidirectional generic sea state spectra are obtained by application of the empirical models for hurricane generates seas by Young (1998, 2003, and 2006), requiring maximum wind speeds, forward velocity and radius to maximum wind speed. An averaged radius to maximum sustained wind speeds, according to Hsu et al. (1998) and averaged forward speed of cyclonic storms are applied in the initial state. In a second step the influence of the forward velocity is investigated and related to the assumption of an extended fetch."*

Conclusion: *"The intention of this desk study was to develop an offshore wind farm site independent sea state, in order to establish the design basis for ULS wave impact study on floating offshore wind turbine foundations. The geographically limited area of interest, where floating foundations are initially likely was lacking respective generic metocean conditions. Based on hurricane wind speeds conceptual deep water extreme design seas states described by spectral parameters were found for a number of geographical areas. Following the parametric procedure outlined by Young (2003, 2006) the hurricane wave spectra values are estimated. The underlying assumption is that the wave generation is fetch limited, though the fetch needs to be described by an equivalent fetch, due to the influence of forward motion of the storm. Wave spectrum parameters have been obtained for the respective maximum sea states found in Figure 4. Table 3 presents the results. For the sake of completeness the obtained significant wave heights have been compared to the integral of the spectral density and only marginal, i.e. negligible, differences have been found. Areas and return periods can be assigned to respective ULS sea states by the help of the wind speed and Table 2. The values outside the validity range are not covered by the table. Weibull distributions have been applied to find maximum sustained wind speeds. The maximum wind speeds obtained for the Japanese east coast are all found to be in Category 2 and 3 for return periods of 50 years and 100 years. The US east coast shows severer*

conditions with Category 4 and 5 for return periods of 50 years and 100 years. Comparing those values to the API Bulletin 2INT-MET (2007) it seems that the current values are conservative. The API Bulletin 2INT-MET (2007), however only gives hurricane design sea states for the Gulf of Mexico, which might be considered worse in terms of occurrence probability. In the Atlantic basin the API RP 2A-WSD (2000), gives for the Baltimore Canyon a 100 year maximum wave height range of 24.4 meter to 30.5 meter and for the Georges Bank, south of Nova Scotia, 22.9 meter to 29.0 meter. Considering Rayleigh distributed waves the maximum wave height can be estimated by simply multiplying the significant wave height with a factor of 1.86. Applying the latter to the 100 year return period Hm0 values of the two northern parts of the US coast, results in a maximum wave height of 29.20 meter. Even though previously stated that the respective values are outside of the validity range, and the two mentioned sites are outside of the investigated corridor the values give some comfort for the overall results. It is found that the applied method reveals slightly higher wave heights in the Atlantic than in the GOM. That is in line with the previously stated assumption. It needs to be emphasized that the found extreme sea states are based on large spatial scale and hence serve as initial input to conceptual offshore structure assessment. All of the above given extreme event sea states are assumed to be conservative for their respective return period. In fact the estimated significant wave heights are assumed to be rather large."

10.1.1 Complimentary Information: Applicability of the results

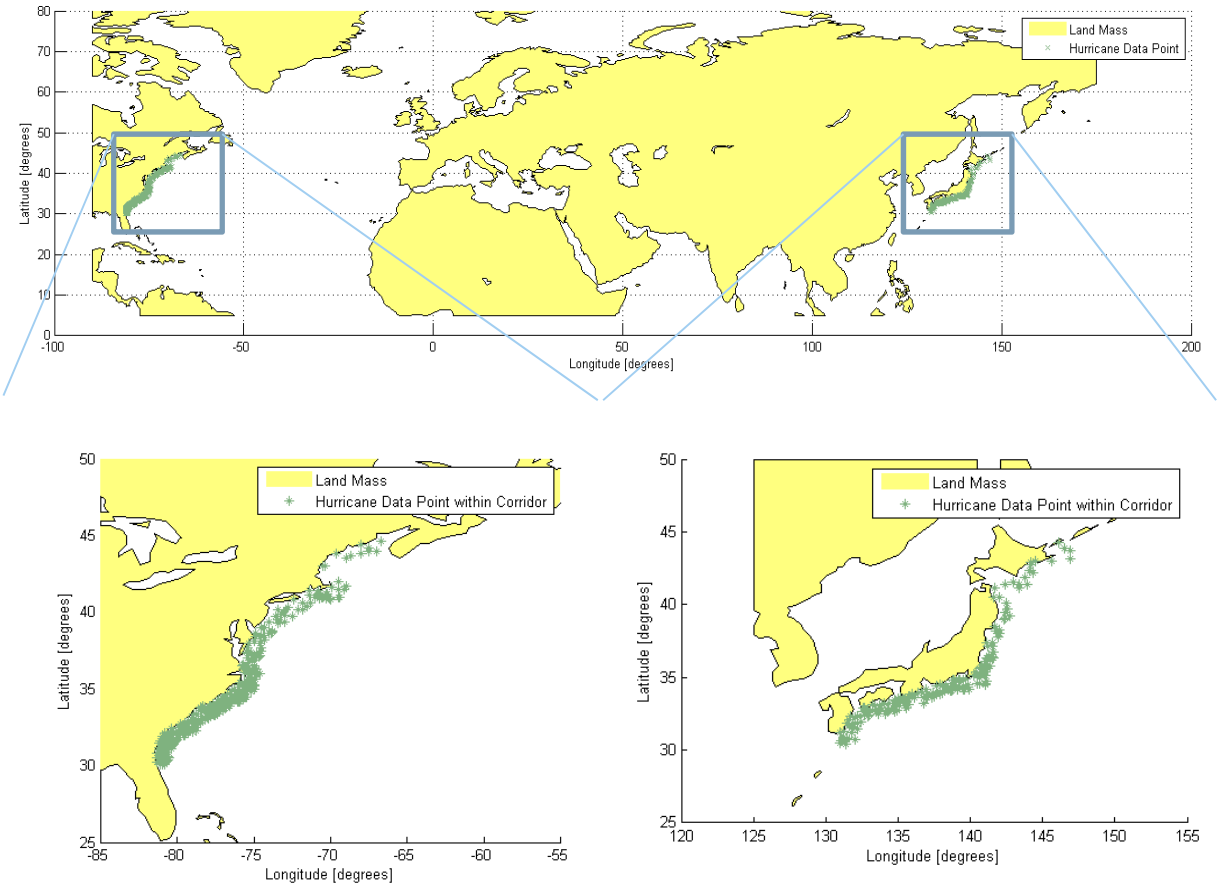

Figure 14: Top Northern Hemisphere Hurricane wind speed data points used for evaluation. Bottom: Enlargements of areas of interest.

A lesson learned from the design sea state development, concerned the rapid development of the industry's focus. In the initial phase of the project, the industry was certain that FOWTs were mainly being built in eastern US waters or eastern Japanese waters. This was why the sea states were based on hurricane measurements along the respective coasts, see Figure 14. The interest as such in these areas has not decreased; an excellent example is the pilot park close to Fukushima. However, three years later, the European market has realised that FOWT should not be discarded as a viable solution for lowering the cost of energy (see also the "Introduction" chapter). This meant that it was important to compare the obtained design sea states from the hurricane assessment to possible sea states in European waters, in order to assess the similarity and applicability. For this the Dogger Bank area was chosen as a benchmark site.

Figure 16 shows the spatial distribution of the H_{m0} values for Design Sea states derived from a wind speed of 30m/s from North West. In the north facing deep areas (50m), Figure 15, it became evident that sea states of up to 12.5m H_{m0} can be expected. Comparing that to the sea states from the parametric study, it seemed sensible to conclude that the lowest parametric study fitted very well to the design sea state at harsh European sites. In order to modify the deep water wave spectrum, characterised by H_{m0} = 12.52m, T_p = 13.66s in >150m depth (see Table 2) , for the intended water depth of ca. 100m, the JONSWAP spectrum was multiplied by a depth function, also known as TMA spectrum, DNV (2010). That resulted in a reduction from H_{m0} = 12.52m to H_{m0} = 12.2m. The above approach was subsequently validated by comparison to a figure presented by Ochi (2003), see Figure 17, which yielded a factor of 0.97 on the 0th moment and hence a very good fit.

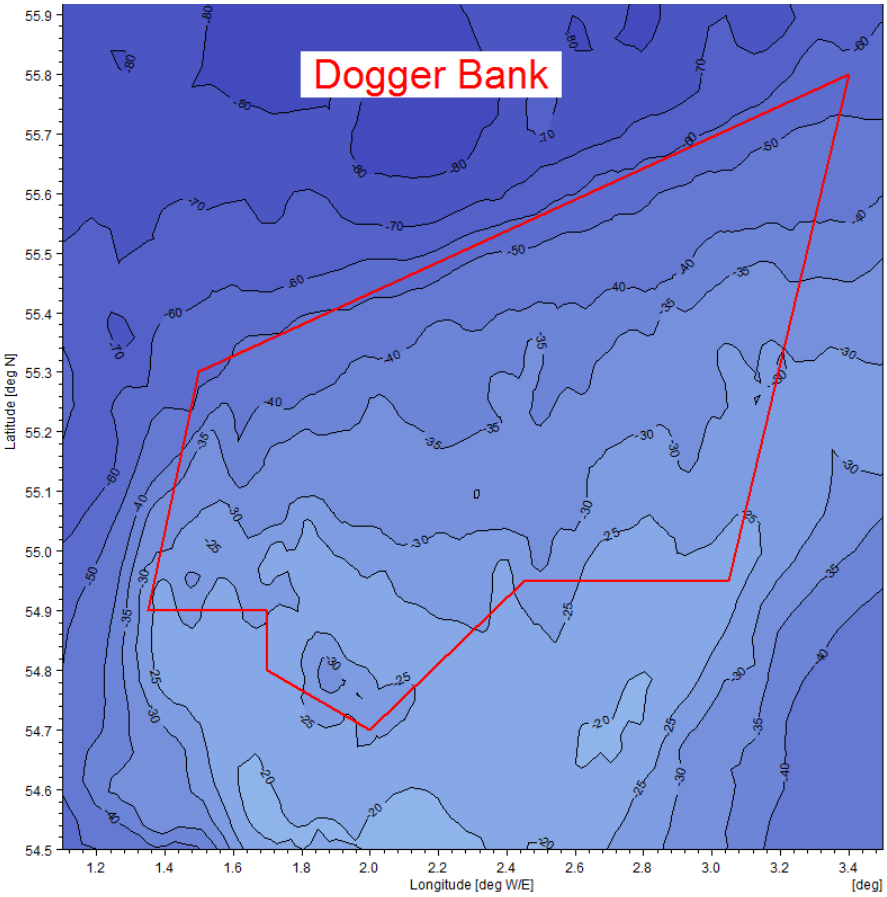

Figure 15: Illustration of the Dogger Bank Offshore Wind Farm area and spatial distribution of the respective water depth w.r.t. LAT spatial distribution - (source: Ramboll Metocean Data Base).

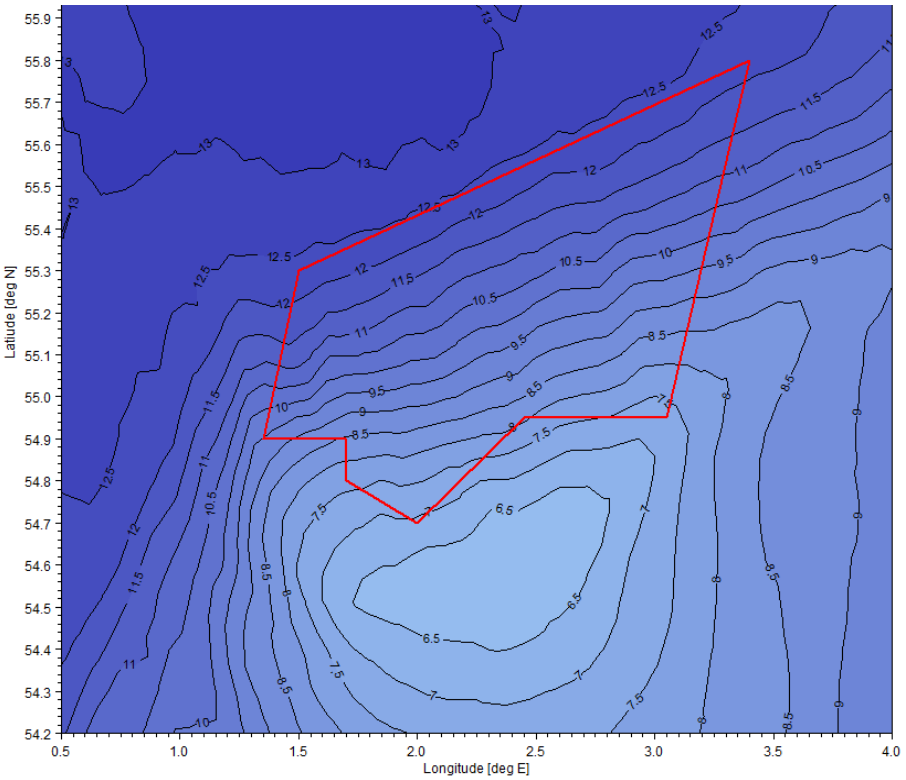

Figure 16: Illustration of the Dogger Bank Offshore Wind Farm area and the respective Hm0 spatial distribution.

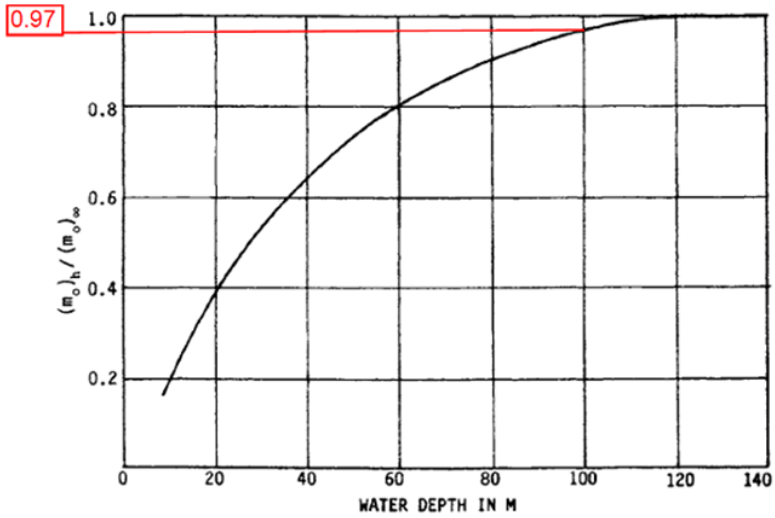

Figure 3.5 – Ratio of area under computed spectrum at a given water depth to that in deep water as a function of water depth.

Figure 17: Indication of obtained ratio, Figure 3.5 taken from Ochi (2003) .

Table 2: Generic Hurricane Sea States from Wehmeyer et al. (2012)

Wind Speed [m/s]	H_{m0} [m]	T_p [s]
44.00	12.52	13.66
45.00	12.79	13.78
51.00	14.33	14.37
52.00	14.57	14.46
53.00	14.80	14.54
54.00	15.03	14.62
56.00	15.46	14.76
61.00	16.44	15.04
62.00	16.61	15.08

It could therefore be concluded that the chosen sea state fulfilled three important requirements:

1. It is a likely sea state being caused by a hurricane
2. It is comparable to European site 50 year return event sea states
3. The wave basin at AAU is capable of generating the respective sea state at a reasonable scale

10.2 Experimental Study of an Offshore Wind Turbine TLP in ULS Conditions (Wehmeyer et al., 2013, Conference Paper)

Abstract: *"An extensive model test program has been carried out in order to assess the behaviour of a tension leg moored substructure as support of a floating offshore wind turbine (FOWT). The floater was inspired by an industrial design. The tests focused on the ultimate limit state (ULS) behaviour, therefore no aerodynamic or gyroscopic effects were included, i.e. the turbine hub was represented by a lumped mass, and focus was given to wave forces and dynamic behaviour. The model tests have been conducted in the 3D deep water basin of the Hydraulics and Coastal Engineering Laboratory at the University of Aalborg at a scale of 1:80. The model tests were made with a range of monochromatic, bichromatic and irregular waves. All waves are modelled long crested and were run with and without sub and super harmonics. Three different structure layouts were tested, i.e. the tests were run with substructure only, with a rigid tower representation and with a flexible tower representation. Three submerged load cells measured the response of the tendons, and two accelerometers measured the response of the total structure, being located at the substructure – tower interface and in the nacelle. The paper intends to describe the setup of the test and presents some selected interim results."*

Conclusion: "*After extensive preparations data gathering has been initiated, in order to gain insights in the importance of ultimate limit state design drivers for a floating offshore wind turbine foundation TLP concept. An industrial inspired TLP structure has been fabricated in model scale with good match between prototype and model realization. The model has been exposed to design environmental conditions. A good quality of the waves was achieved; however a detailed run by run assessment has not yet been carried out. It can already be stated, that the disturbances due to reflected waves is very low. Consequently that indicates a good performance of the wave tank absorption system, as well as low reflection of the structure, i.e. it might be regarded as hydrodynamic transparent. It can be concluded that the required data on the system's motion response is not disturbed by noise being caused by reflected waves. Early stage data assessment of the loading side, i.e. laboratory waves, as well as of the response side, i.e. tendon loads and high frequency accelerations, has been carried out. Results are in accordance with findings from numerical studies and give confidence in the overall data quality. Deviations have been identified on the loading side, comparing the intended and achieved wave realizations, which now need to be considered in the subsequent analysis. It can generally be stated that the inclusion of 2nd order wave harmonics in wave generation is essential and is recommended to be considered. For the extreme events, a purely linear wave generation, which leads to spurious uncontrollable waves, generated a significantly different structure response than one including at least 2nd order wave harmonics. The presented extensive wave grid, ranging from rather small regular waves to large irregular waves, will allow to assess the significance of in-or excluding the 2nd order wave harmonics. Hence further work will be done in identifying differences in the responses also in monochromatic and bichromatic waves. It can already be stated that the inclusion leads to an increase of ringing response as well as in an increase in the number of slack line events and corresponding tendon/anchor compression. It is currently not clear if this compression is a real effect or a consequence of the model setup. Slack line events have been reported. It is a common state-of-the-art to design TLP structures such that slack line events do not occur, even in the most extreme cases. However, that is mainly due to the fact that the tendons of traditional TLPs' are made of steel tubes, which do not allow buckling leading to failure. Applying however chains or polyester lines, the design focus is moved towards the connection points, which can be designed respectively. An effect of sea state maturity could be identified on the number of slack line events and on the standard deviation of the ringing response. Additionally it has been found that the effect of increasing wave non-linearity and top side flexibility affects the acceleration in fore-aft direction at nacelle level in actual value and number of events."*

10.2.1 Complimentary Information: Observations after the model tests

The model was placed over the deep section, which enabled correct length scaling of the tendons. A cover plate was installed over the deep section to ensure continuous water depth and hence the deep section had no influence on the waves, see Figure 18.

Figure 18: Deep section with cover plat, in dry conditions.

However, the combination of a deep section and the generation of a rather large sea state in front of the wave paddle challenged the non-breaking wave height generation. The intended significant wave heights were 0.1528m and a period of 1.53s. In combination with a water depth of 0.697m this results in an Hm0/Depth ratio of 0.22, which implies some wave breaking and hence energy loss. The wave breaking was in line with the observation. The mean of the obtained wave heights was 0.1390m with a peak period of 1.55s.

10.3 Validated hybrid model of a TLP including a flexible topside in non-linear regular waves (Wehmeyer et al., 2014, Journal Paper)

Abstract: *"Extensive model tests have been carried out with a three legged tension leg platform (TLP) supporting an Offshore Wind Turbine (OWT), and have been reported earlier, Wehmeyer (2013). The model tests have been carried out with both a rigid and a flexible topside structure. It was intended to validate a three degree of freedom (3DOF) numerical time domain code including coupling terms, which is described in the following. The idealised structure had lateral symmetry, in the x-z plane, which consequently means surge, heave and pitch were uncoupled from sway, roll and yaw. The numerical results were compared to the physical model test data from non-linear regular waves for both structural layouts. Furthermore was the developed solver benchmarked for selected cases against the commercial hydrodynamic 3d panel code ANSYS AQWA. The developed time domain solver used the linear hydrodynamic coefficients obtained from ANSYS AQWA and a state space approximation of the retardation kernel. Tethered mooring effects and additional dispersive terms, i.e. drag forces from viscous fluid effects were included. The latter were determined from the non-linear drag part caused by the relative velocity between the structure and an incident non–linear wave. The flexible topside structure has been fully integrated in the time domain model by a two element beam model and a lumped top mass. The mass of the wind turbine blades were included in the lumped top mass. The wind induced loading is at the current stage not considered, as the investigation aims validate the hydrodynamic response."*

Conclusion: *"Non-linear waves are assumed to be relevant in the ULS analysis of FOWTs installed close to the minimum target water depth of 50 m. The intention was to set up a resource-efficient tool, able to satisfactorily approximate pitch motions of a dynamically-sensitive FOWT resulting from a nonlinear wave impact. As a numerical experiment, a hybrid model was developed, including linear potential theory forces and non-linear hydrodynamic viscous forces. The potential forces act thereby on the large volume part of the structure, whereas the viscous forces act on the cylindrical surface piercing part of the structure. Due to the violation of the potential flow approximations induced by wave non-linearity, the hybrid model needs to be validated by experimental tests. The CD values applied in the hybrid model are used as tuning parameters. Considering*

that these are in sensible ranges, the overall match between the observations and the hybrid model is very good. To the authors' knowledge, this is the first time a mildly-nonlinear approach has been assessed, comparing measured pitch responses to observed pitch responses excited by non-linear waves based on Stream-function theory. The term mildly-nonlinear describes the combination of linear radiation and wave scattering combined with additional non-linear terms, assuming small body motions. It was shown that the viscous drag contributions are an essential part of the response for the investigated structure, and it seems sensible to include those effects, as well, in subsequent irregular wave response analysis. Additionally, a code-to-code comparison was carried out and served as the performance verification for non-flexible topside configurations. It was shown that the hybrid model can be adopted to deliver more than satisfying results for different wave steepness values and different topside flexibilities. The model is thereby able to:

- *Include the effects of regular, non-linear waves on an FOWT TLP structure;*
- *Include the effects of the dynamically-sensitive topside on the pitch response of an FOWT.*

Comparing the maximum pitch values obtained by the rigid body simulation to those of the flexible topside simulation, the impact of the rigid body assumption becomes evident. Even though this appeared to be very structure specific, it underlines the importance of the correct implementation and furthermore proves that the rigid body assumption inherited from the O&G industry is not valid for FOWTs. It was not expected to obtain perfect fits, due to the complexity of the system and due to the simplifications. A higher fidelity model could be achieved by inclusion of the nonlinear Froude–Krylov force. When simulating irregular waves, second order diffraction forces might become relevant. However, the non-linear viscous contributions are expected to be of the same or higher significance, especially in severe seas for surface piercing parts, which are drag dominated. Considering the lateral extent of the structure, an integration of the instantaneous drag contribution over the wetted surface might lead to further improvement. However, the results already showed good agreement with the measured data. It is thereby concluded that the applied methodology is robust enough to be developed further. A natural next step is the assessment of key responses in irregular waves. Even though the general approach seems valid, a current limitation, and, therefore, incentive for future work, is the specific applicability of the model. Exchanging the potential flow coefficients is not a major challenge; however, the current drag coefficient implementation and the current mooring model makes the model case specific. Further development work, in order to make the model more generally applicable, i.e. acceptable for different substructures and mooring configurations, is consequently planned.

10.3.1 Complimentary Information: Technical implementation of the hybrid TLP model

The TLP FOWT was represented by a 5DOF hybrid model, which had lateral symmetry in the x-z plane, meaning surge, heave and pitch were decoupled from sway, roll and yaw. Due to this and due to long crested wave impact, a two dimensional model was assumed to be sufficient. The 5DOF equation of motion was solved at the connection point of the tower bottom and the substructure, TB. An exaggerated system description is given in Figure 19.

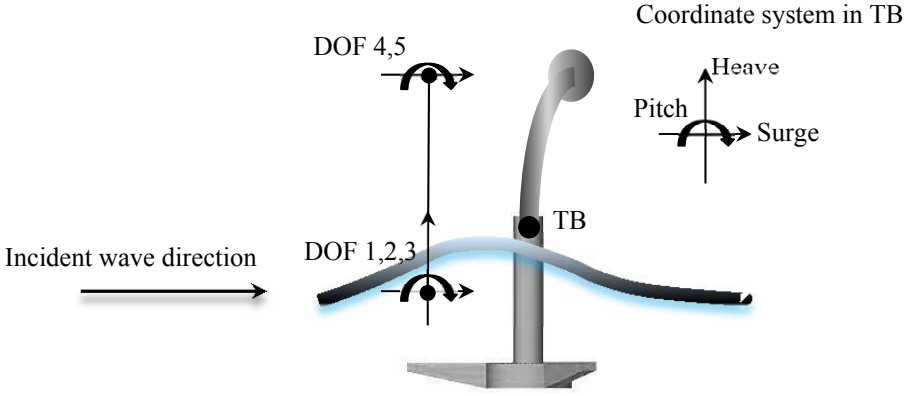

Figure 19: Illustration of reference system, nonlinear wave and FOWT with flexible topside.

10.3.2 Complimentary Information: Mass and stiffness matrices

Table 3: Mass and stiffness matrices for the beam element and the floater.

Illustration of the 2 transverse and 2 rotational beam nodes	Mass matrix	Stiffness matrix
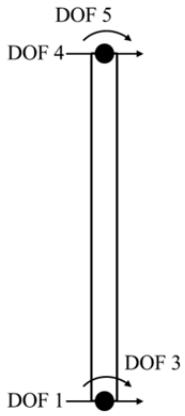 Note: The DOF are already numbered according to the 5 DOF system	$M_{Topside} = \frac{M_{Tower}}{420} * \begin{bmatrix} 156 & 22l & 54 & -13l \\ 22l & 4l^2 & 13l & -3l^2 \\ 54 & 13l & 156 & -22l \\ -13l & -3l^2 & -22l & 4l^2 \end{bmatrix} + \begin{bmatrix} 0 & 0 & 0 & 0 \\ 0 & 0 & 0 & 0 \\ 0 & 0 & TM & 0 \\ 0 & 0 & 0 & 0 \end{bmatrix}$ Extended to a 5DOF system: $M_{Topside} = \frac{M_{Tower}}{420} * \begin{bmatrix} 156 & 0 & 22l & 54 & -13l \\ 0 & 0 & 0 & 0 & 0 \\ 22l & 0 & 4l^2 & 13l & -3l^2 \\ 54 & 0 & 13l & 156 & -22l \\ -13l & 0 & -3l^2 & -22l & 4l^2 \end{bmatrix} + \begin{bmatrix} 0 & 0 & 0 & 0 & 0 \\ 0 & 0 & 0 & 0 & 0 \\ 0 & 0 & 0 & 0 & 0 \\ 0 & 0 & 0 & TM & 0 \\ 0 & 0 & 0 & 0 & 0 \end{bmatrix}$ Eq. 10	$K_{Topside} = \frac{EI}{l^3} * \begin{bmatrix} 12 & 6l & -12 & 6l \\ 6l & 4l^2 & -6l & 2l^2 \\ -12 & -6l & 12 & -6l \\ 6l & 2l^2 & -6l & 4l^2 \end{bmatrix}$ Extended to a 5DOF system: $K_{Topside} = \frac{EI}{l^3} * \begin{bmatrix} 12 & 0 & 6l & -12 & 6l \\ 0 & 0 & 0 & 0 & 0 \\ 6l & 0 & 4l^2 & -6l & 2l^2 \\ -12 & 0 & -6l & 12 & -6l \\ 6l & 0 & 2l^2 & -6l & 4l^2 \end{bmatrix}$ Eq. 11
Illustration of the two transverse and one rotational floater nodes	Mass matrix of the Floater at COG	Stiffness matrix of the Floater at COG
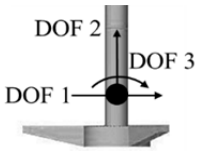	$M^{COG}_{Floater} + mh^{COG}_{Floater} = \begin{bmatrix} M_{11} & 0 & 0 \\ 0 & M_{33} & 0 \\ 0 & 0 & J_{55} \end{bmatrix} + \begin{bmatrix} mh^{COG}_{11} & mh^{COG}_{13} & mh^{COG}_{15} \\ mh^{COG}_{13} & mh^{COG}_{33} & mh^{COG}_{35} \\ mh^{COG}_{15} & mh^{COG}_{35} & mh^{COG}_{55} \end{bmatrix}$ Eq. 12 Note: Indices in equation Eq. 12 are in accordance with common floating structure notations: 11 = Surge, 33 = Heave, 55 = Pitch	$K^{COG}_{Floater} = \begin{bmatrix} 0 & 0 & 0 \\ 0 & K^{COG}_{33} & K^{COG}_{35} \\ 0 & K^{COG}_{35} & K^{COG}_{55} \end{bmatrix}$ Eq. 13 Note: Indices in equation Eq. 13 are in accordance with common floating structure notations: 11 = Surge, 33 = Heave, 55 = Pitch

With:
$M_{Topside}$ = Mass matrix of the tower and RNA

M_{Tower} = Mass of the tower [kg]

l = Length of the tower [m]

TM = RNA mass [kg]

$K_{Topside}$= Structural stiffness matrix of the tower

EI = Bending stiffness of the tower [Nm^2]

$M_{Floater}^{COG}$= Mass matrix of the floater

$mh_{Floater}^{COG}$ = Added mass matrix of the floater

$K_{Floater}^{COG}$ = = Hydrostatic stiffness matrix of the floater

The topside mass and stiffness were included by using a single-finite-element model of a linear elastic Bernoulli beam, Table 3. The respective derivation of the mass and stiffness matrices for a 2 node beam element can be found in several text books and is not repeated here, e.g. Næss (2013). The RNA mass, i.e. top mass (TM) was added in the 3rd DOF of the beam. The four degree of freedom (4DOF) beam element was subsequently coupled to the transformed (from the rigid body centre of gravity to TB, see section 10.3.6) rigid body terms for surge, heave and pitch in the mass, stiffness and damping matrices, by summation of their terms in the shared DOFs, where the mass in heave, i.e. DOF 2 of the rigid body contained already all heave relevant masses.

10.3.3 Complimentary Information: Structural damping

The structural damping matrix $C_{Topside}$ of the tower nacelle assembly was included by Rayleigh damping where

$$C_{Topside} = \alpha_1 M_{Topside} + \alpha_2 K_{Topside} \quad \text{Eq. 14}$$

Where α_1 & α_2 were given by:

$$\alpha_1 = \frac{2\omega_1\omega_2}{\omega_2^2 - \omega_1^2}(\zeta_1\omega_2 - \zeta_2\omega_1) \quad \text{Eq. 15}$$

$$\alpha_2 = \frac{2(\zeta_2\omega_2 - \zeta_1\omega_1)}{\omega_2^2 - \omega_1^2} \quad \text{Eq. 16}$$

Where ω_1 & ω_2 were the structural frequencies calculated from on $M_{Topside}$ and $K_{Topside}$. and ζ_1 & ζ_2 were the structural damping values for the first and second eigenmode.

It was found that the connection between the topside was not as stiff as originally intended. The measured topside bending stiffness values and structural damping ratios could therefore not be applied. Both parameters however served as tuning parameters in the response model, i.e. decay with no wave excitation. For further information it is referred to section 10.3.10.

10.3.4 Complimentary Information: Radiation damping

The motion of the floater generates waves, which generally speaking will influence the floater's motions in return. This is called the fluid memory effect, which is considered by the convolution integral, which is a function of the so called retardation function or retardation kernel C^{rad} . The latter is a causal unit impulse

response function for each DOF and respective coupling terms. By applying Ogilvie's formula, Ogilvie (1964), C^{rad} as well as the added mass at infinity value mh_{ij}^{COG} can be obtained from the frequency domain radiation damping coefficients and the frequency domain added mass coefficients, see for instance Fossen (2011). To reduce computational expense a state-space model was used instead of the convolution function to compute the radiation damping force vector μ^{COG} in the time domain. Several references for this could be found, e.g. Duarte et al. (2013), Kristiansen et al. (2005) and Perez and Fossen, (2009). All of them refer or describe the MSS FDI MATLAB toolbox, which was as well applied in the current work to obtain the time invariant state space representation and the added mass at infinity values (in a time variant state space representation the matrices would be a function of time). The MSS FDI MATLAB toolbox uses a least square method to estimate the transfer function directly by a so called frequency domain identification, from which the state space matrices A, B, C and D are obtained.

For a coupled 3 DOF system and as the order of the transfer function chosen in this application to be three, this yielded to 27 state variables. In general, a state describes the condition of the system at a certain point in time due to an input, and the resulting force is how the system reacts to a given input, due to the particular condition, or state. Both descriptions of the radiation damping force are given in Eq. 17 and Eq. 19. The impulse response functions of the radiation force for the rigid body motions and their respective state space representations are shown in Figure 20.

$$\mu^{COG} = \int_0^t C^{rad}(t-\tau)\, \dot{x}\ (\tau) d\tau \qquad \text{Eq. 17}$$

$$\dot{\xi} = A\ \xi + B\ \dot{x} \qquad \text{Eq. 18}$$

$$\mu^{COG} = C\ \xi + D\ \dot{x} \qquad \text{Eq. 19}$$

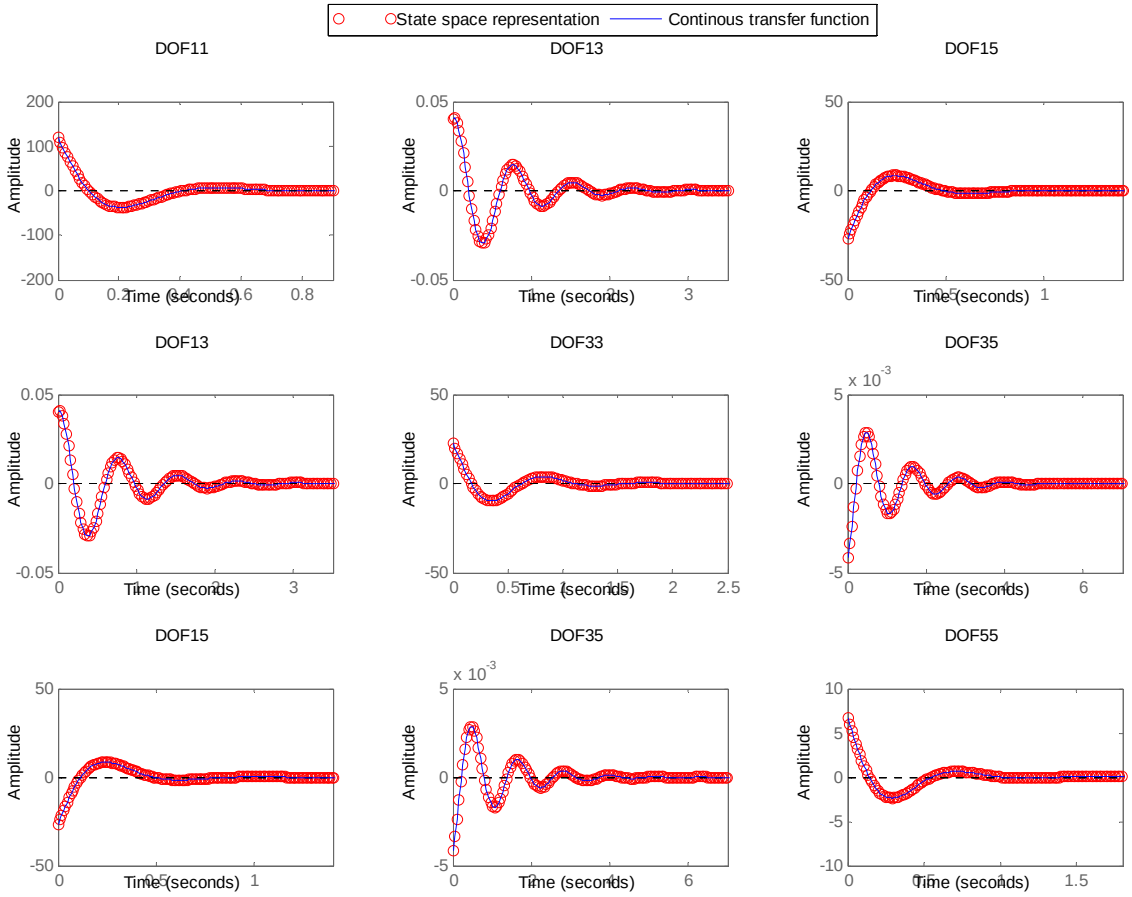

Figure 20: Fit of state space representations of the radiation damping impulse response functions. Note: Indices in Figure 20are in accordance with common floating structure motions: 1 = Surge, 3 = Heave, 5 = Pitch.

10.3.5 Complimentary Information: Benchmarking of State Space approach

Before applying the state space approximation approach to the more complex TLP model, the approach was verified by comparing lab test data of a floating hemisphere against a respective 1DOF equation of motion solver, which is not further described here. The structure was exposed to a mild irregular sea state, which thereby could be regarded as linear. The wave elevation was measured next to the structure. Consequently, the surface elevation signal could be used for the generation of the excitation force, and enabled direct comparison between the observed rotation and the numerical simulation. Figure 21, shows a part of the time series, comparing the measured rotation against the predicted rotation. The fit between the two signals is very satisfying and the application of a state-space approximation for the fluid memory effect was validated.

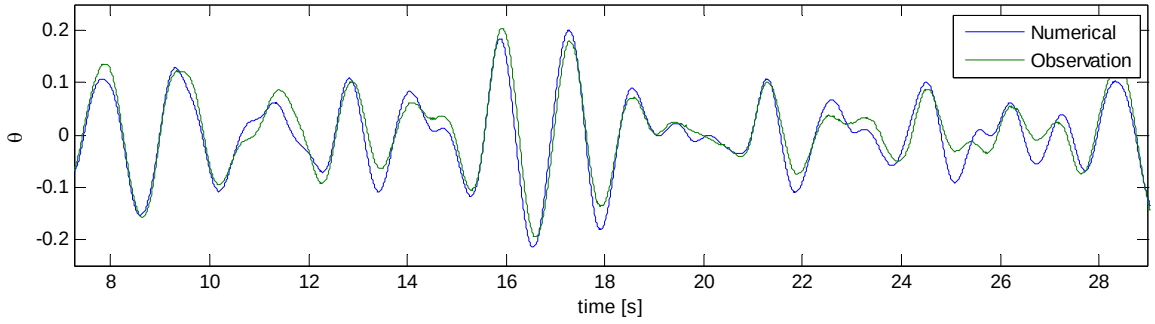

Figure 21: Benchmark test of state space approach, using the measured rotation of a floating hemisphere in a linear irregular sea state.

10.3.6 Complimentary Information: Transformation from COG to TB

The equation of motion needed to be solved at the interface between the tower and substructure (TB). The rigid body inertia matrix, rigid body stiffness matrix, rigid body damping matrix and excitation forces were therefore transformed from their origin to TB.

For the floater the origin was located at its COG, i.e. where the seakeeping program ANSYS AQWA calculated the hydrodynamic coefficients. The vector $r_{COG} = [x_{COG}, y_{COG}, z_{COG}]^T$ was the distance vector from the point of interest, i.e. interface point TB, to the calculation point COG.

For a 6DOF system transformation matrix can then be written as

$$H(r_{COG}) = \begin{bmatrix} I_{3x3} & S^T r_{COG} \\ 0_{3x3} & I_{3x3} \end{bmatrix} \quad \text{Eq. 20}$$

Where I_{3x3} was the identity matrix and

$$S^T r_{COG} = \begin{bmatrix} 0 & r_3 & -r_2 \\ -r_3 & 0 & r_1 \\ r_2 & r_1 & 0 \end{bmatrix} \quad \text{Eq. 21}$$

Where r_i refers to the entries in r_{COG}.

In the current application the transformation matrix was reduced to 3DOF according to the 2D assumption. Exemplarily, the transformed inertia matrix can then be obtained as in Eq. 22

$$H^T(r_{COG}) \;\; M^{COG}_{Floater}\, H(r_{COG}) = M_{Floater} \quad \text{Eq. 22}$$

The approach followed in the present work can be found in more detail in Fossen (2011).

10.3.7 Complimentary Information: Hydrodynamic viscous drag forces

The linear inertial part of the wave excitation was described in section 9 and presented in Figure 12. The frequency domain wave excitation coefficients have been determined with the potential flow solver ANSYS AQWA (2013). In order to account for the drag part of the wave excitation, idealised waves, realised by Stream-function wave theory, Fenton (1988), have been adjusted to the experimental waves, and subsequently applied in the numerical model, see Figure 22.

From the computation of the Stream-function wave, the wave elevation, the horizontal and vertical kinematics were imported and interpolated onto the respective time step of the solver.
The viscous drag forces were calculated section wise vertically along the structure by the drag part of Morison's equation, Eq. 3, considering the instantaneous relative velocities between the respective wave kinematics and the rigid body kinematics. The resulting forces and moments were calculated with respect to the COG of the substructure and as well transformed to the point of interest TB.

A more thorough investigation of the drag load regime, including model tests, would be recommended in order to deepen the understanding and provide the basis for a more general implementation. At the current stage, the hybrid model is tuned to fit the investigated structure exclusively.

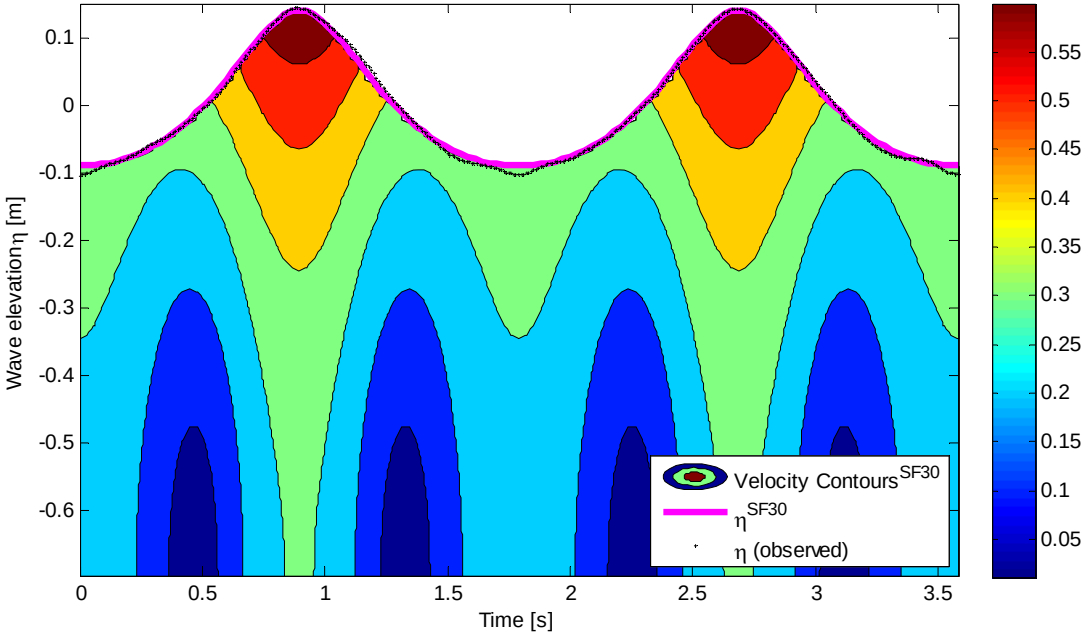

Figure 22: Observed wave elevation and corresponding Stream-function wave fit including absolute particle velocity contours, for a regular non-linear wave.

10.3.8 Complimentary Information: Equation of Motion

The final equation of motion needed to couple the topside and the floater. Therefore was the four degree of freedom (4DOF) beam element subsequently coupled to the transformed (from the rigid body centre of gravity to TB) rigid body terms for surge, heave and pitch in the mass, stiffness and damping matrices, by summation of their terms in the shared DOFs, where the mass in heave, i.e. DOF 2 of the rigid body contained already all heave relevant masses. The resultant hybrid model was in essence a time domain solver of the equation of motion, with the following force contributions:

$$\left(M_{Topside} + M_{Floater} + mh_{Floater}\right)\ddot{x}(t) + \mu + \left(K_{Floater} + K_{Topside}\right)x(t) + F_{Mooring} + C_{Topside}\dot{x}(t) = F_{Exc\_inertial} + F_{Exc\_viscous\ drag} \quad \text{Eq. 23}$$

The left hand side described the body motion by:

- $\left(M_{Topside} + M_{Floater} + mh_{Floater}\right)$ = Combined mass matrix, consisting of the topside mass matrix, the transformed substructure mass matrix and the transformed added mass matrix
- μ = Transformed hydrodynamic radiation damping force vector, where the State-space system was solved simultaneously to the equation of motion, Eq. 23
- $\left(K_{Floater} + K_{Topside}\right)$ = Combined stiffness matrix, consisting of the transformed hydrostatic restoring matrix and the stiffness matrix of the topside
- $F_{Mooring}$ = Transformed station keeping force vector
- $C_{Topside}$ = Damping matrix of the Topside
- x = Displacement vector

The right hand side described the excitation force by:

- $F_{Exc\_inertial} + F_{Exc\_viscous\ drag}$ = Wave excitation force vectors, consisting of the transformed inertial

(Froude-Krylov force and diffraction force) vector and the transformed viscous drag force vector

10.3.9 Complimentary Information: Model validation in small waves

The numerical model of the TLP FOWT was subsequently validated against responses from a small incident wave. The wave excitation was purely inertial but viscous damping was considered. Only one tower layout was investigated, as it was assumed that in very small waves the influence of the tower flexibility was negligible. Figure 23 shows the comparison for the stiff tower layout. By visual inspection, it was concluded that the numerical model predicted the responses well.

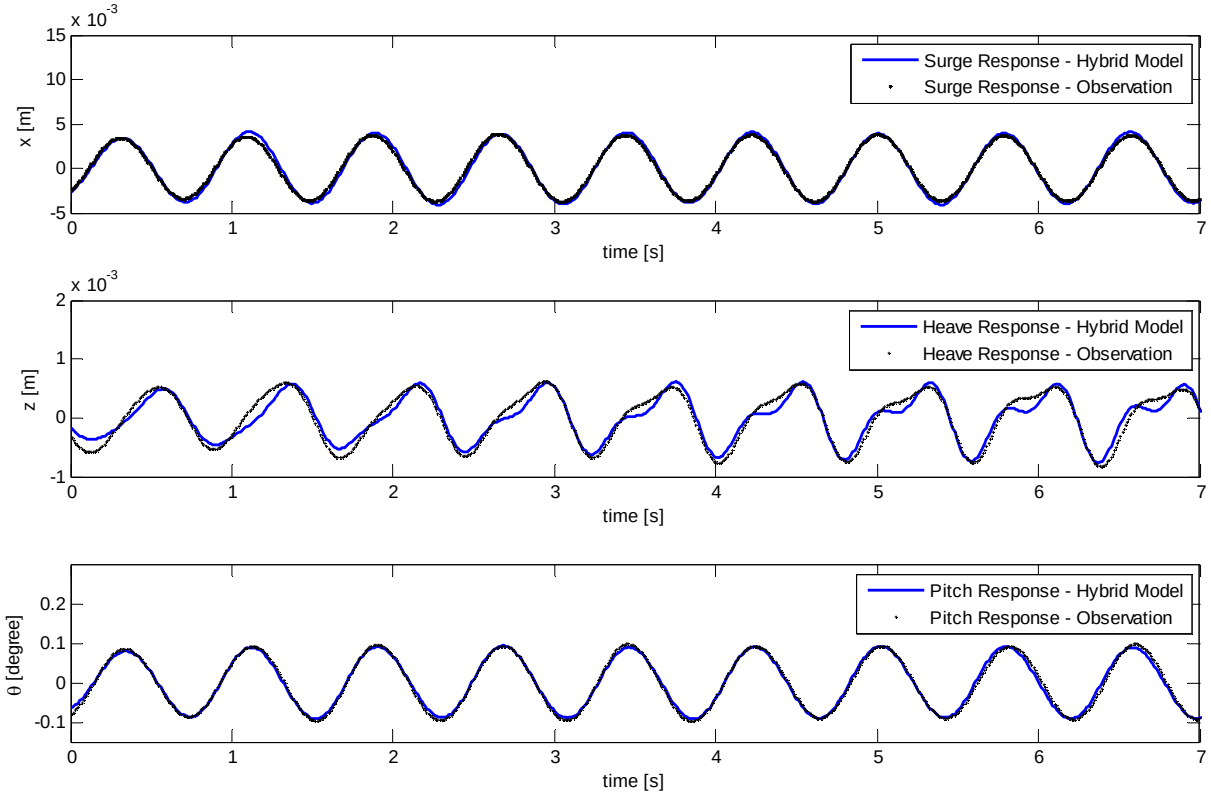

Figure 23: Comparison of measured responses and predicted responses for the three degrees of freedom, for small incident wave.

10.3.10 Complimentary Information: Progressive weakening – physical model deterioration

The benchmarking of the numerical model against ANSYS AQWA showed very satisfying agreement for the pitch decay test and the pitch response in regular waves. For this it was required to increase the bending stiffness of the beam element by an order of magnitude, in order to resemble a fully rigid body, i.e. rigid floater plus rigid topside. However, the numerical model over predicted the natural frequencies for the stiff tower and the flexible tower. As it was known from Matha (2009) that the natural frequencies for flexible topsides are lower than for rigid topsides (in pitch) the natural frequencies for the three different layouts were compared.

It was found that the natural frequency of the initially stiff topside was actually located in between those of the flexible topside and the rigid body results, though the initial intentions was a rigid body representation by using a very stiff material for one of the physical topsides. Investigating the physical model subsequently showed a dramatic weakening of the connection point at the interface of tower and substructure. Obviously this meant a change in natural frequency and damping. As by that time the model was already in a suboptimal state, measuring of the actual bending stiffness was not any longer possible. The most straightforward approach to account for this was tuning of the numerical EI and the numerical damping, based on pitch decay tests and consequently fixing the parameters for the subsequent numerical models. The change was dramatic

and it was discovered that the connection most probably experienced progressive weakening. For the flexible topside a value of 27 Nm^2 was required, a decrease of 36% from the original 75Nm^2. For the rigid topside the required change was found to be more significant. A decrease from 850Nm^2 to 37 Nm^2 along with a further decrease of 10% was needed for the comparison between the numerical model and observations that had been performed consecutively. This indicates that the connection point was the crucial point. However, the application of the adapted bending stiffness values delivered more than satisfying agreements when the numerical results were compared to the observations. Furthermore very satisfying agreement was found in the benchmark studies against the rigid body simulation tool ANSYS AQWA, where the influence of the connection was eliminated and therefore validated the hybrid model. An important finding of this was that the importance of interface connection, which hence needs special attention. Not only in future physical model testing (for example has the experience has already been passed on to another project – InnWind.eu[1]) but also in full scale applications.

10.4 Mooring response of a floating offshore wind turbine in nonlinear irregular waves (Wehmeyer and Rasmussen, 2014, submitted Journal Paper)

Abstract: "*The current work focusses on the mooring loads obtained by a numerical model of a floating offshore wind turbine foundation (FOWT), where the substructure is a three legged Tension Leg Platform (TLP) concept. Representatively, the behaviour of one tendon is investigated. The FOWT is represented by a hybrid model, which includes a flexible topside and which combines the linear inertial excitation forces, obtained by potential flow, with the non-linear hydrodynamic viscous drag forces. The latter are obtained from the relative velocities between nonlinear sea state kinematics and the floater. The nonlinear sea state surface elevation and kinematics are generated by a second order wave model, including all sub- and super-harmonics, with and without an embedded stream function wave, which replaces the highest randomly generated wave with a predefined design wave. The numerical responses are compared to observations from model tests and the applicability for engineering purposes is briefly discussed.*"

Conclusion: "*Not surprisingly, the higher order irregular wave generation is well established and good agreement can be seen between the distributions of numerical results and measurements. The embedment of a stream function wave is a common industry practice, it needs however to be defined as an engineering approach and to the author's knowledge, it is the first time that an embedded stream function wave is used as an incident wave for a FOWT. The approach is certainly controversial, due to the violation of linear theory. It is however not so much the intention to accurately depict the observed responses – the intention is much more to assess how a rather simple numerical hybrid model reacts if exposed to nonlinear wave elevations and kinematics. The fundamentally new challenge of installing dynamically sensitive FOWTs in limited water depth will in the short term future require clarification on the applicability of time efficient solutions for respective design tasks. The current work intends to assess if at all it is possible and which degree of conservatism the approaches inherits. The irregular incident wave runs over predict the measured maximum loads by on average 32%, where the non-linear irregular wave runs yield to the more conservative load ratios. From there it can be concluded that the linear irregular incident wave is sufficiently conservative even though the non-linear incident wave model resembles the surface elevation better (and probably also the wave kinematics). The embedded wave approach results in slightly lower overall averaged maximum loads, i.e. an over prediction of 29%.*

Based on the current status, it is therefore concluded that the latter provides the most controlled and time efficient engineering tool, though still conservative. The background sea state is better resembled by the higher order model and simultaneously the highest wave is distinctly defined. Therefore, the approach might also be used to investigate high frequency responses from ULS transient effects and slack line events especially for TLP structures. However, since the incident waves can be assumed well defined, a higher fidelity structural model is required, in order to match the measured results better and therefore decrease the conservatism."

[1]innwind.eu - innovative wind conversion systems (10-20MW) for offshore applications, EU 7th Framework Grant agreement No.308974

10.4.1 Complimentary Information: Slack line events

A thorough investigation of so called slack-line events was not any longer possible within the scope of the current work. However, some preliminary results are presented to point out further areas of interest and strengthen the conclusion. For a TLP structure slack-line events are highly critical. The tendons and the respective connection points are designed for constant tension. If the motion of the structure becomes larger than predicted, the tendons might lose their pre-tension. The subsequent re-tensioning is accompanied by a snap-load event, which induces critically high impacts on the whole tendon system.

The number of slack line events observed and predicted by the irregular wave runs is shown in Table 4. As expected, the non-linear irregular incident wave runs resulted in a higher average number of slack line events than the linear irregular incident wave run. The highest γ value resulted in the highest number of slack line events for both realisations, which was unexpected considering that sea state steepness values decrease with increasing γ value. It was assumed that an expected trend would be found by a higher number of runs. Both numerical realisations under predicted the number of slack line events.

The incident embedded Stream-function waves always resulted in slack line events. This was expected, as all of the realisations included the maximum measured wave. It was observed, that the slack-line events were caused by the troughs in front of the embedded waves. A high frequency impact response in the tendon around the heave natural frequency 2.5Hz could be seen after the embedded wave, Figure 24. This could be expected as well, even though no special steep wave impact model has been used. The high frequency response caused a subsequent second slack line event occurring after the embedded wave in most of the cases. These observations are not further discussed; however intend to highlight the need for a parameter study on the embedment approach of the Stream-function wave. Additionally, it is suggested to study different wave impact models and verify them by further physical model test campaigns, focussing on the extreme limit state events.

Table 4: Slack-line events of numerical simulations and observation

γ	1.25	2.5	4.48	Mean
Mean 1st Order	2	3	5	3
Mean 2nd Order	4	4	6	5
Observed	9	7	4	7

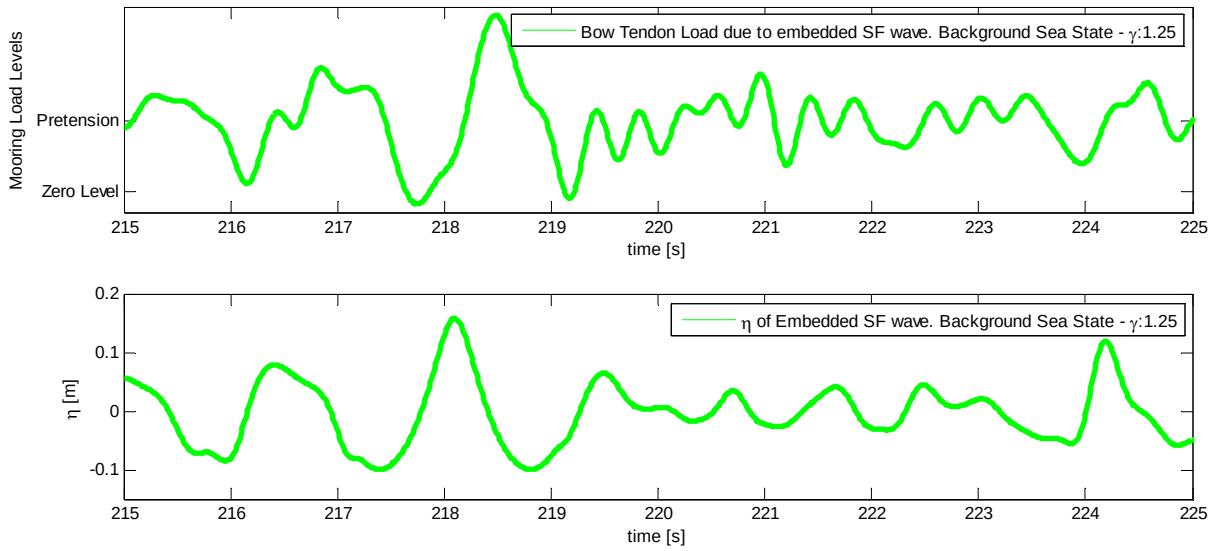

Figure 24: Top: Excerpt of bow tendon load response to incident embedded Stream-function wave. Bottom: Non-linear irregular sea state surface elevation with embedded Stream-function wave.

Finally this highlights, that the embedded wave approach provides a controlled measure to assess critical events also for FOWT. A solid engineering approach however requires further developments, in order to obtain a better match with the measured results and decrease conservatism.

10.5 Resume of the individual conclusions

For the assessment of a FOWT TLP in ULS conditions, a generic extreme sea state was required in order to cover cyclonic storm conditions. It was concluded that the developed sea state was comparable to a 50 year return period event sea states at a harsh European site. The sea state could be simulated in the 3D wave basin of the Aalborg University allowing a reasonable model scale, i.e. 1:80.

A physical TLP FOWT model was subsequently manufactured and equipped with topsides of different flexibilities. The model test campaign delivered floater responses in an extensive wave grid, ranging from rather small regular waves to large irregular waves. This allowed subsequent validation of a numerical model. The developed numerical hybrid model delivered more than satisfying results in regular non-linear waves matching the measured pitch values for a flexible topside layout as well as for a stiff topside layout.

From the 50 year return period event sea state, the measured bow tendon loads were compared to those predicted by the hybrid model exposed to the respective numerical sea state. It was shown that the hybrid model overestimated the highest 5% - 10% of the measured bow tendon loads with about 30%. Applying linear irregular incident waves lead to 32% overestimation, non-linear irregular incident waves lead to 34% overestimation while and non-linear irregular incident wave with a pre-defined maximum embedded Stream-function wave lead to 29% overestimation.

Considering that the surface elevation (and probably also the wave kinematics) were well represented by the higher order wave model, it highlighted the need for further development. Especially the higher order inertial forces could not be covered by the present setup, and should subsequently be included. It was shown that the inclusion of higher harmonics in the physical wave generation delivered a higher number of slack lines. This trend could as well be seen in the hybrid model. However, the number of events was larger in the physical model.

It was briefly shown that in the hybrid model an embedded Stream-function wave ensured a slack line event around the maximum wave and a subsequent high frequency response in the tendons. It is therefore concluded that the embedded wave method provides an engineering tool, which enables the assessment of FOWT responses in non-linear wave conditions, though improvements are necessary to reduce the conservatism.

11. REFERENCES

Agarwal, P. and Manuel, L. (2010), "Incorporating Irregular Nonlinear Waves in Coupled Simulation of Offshore Wind Turbines," 48th AIAA Aerospace Sciences Meeting Including the New Horizons Forum and Aerospace Exposition, Orlando, Florida.

ANSYS AQWA Manual, (2013). Release 15.0.

Bachynski, E. E., Moan, T., (2012), "Linear and nonlinear analysis of tension leg platform wind turbines", In Twenty-Second International Ocean and Polar Engineering Conference, Rhodes, Greece, Vol. 1, pp. 240{247, no. 2012-TPC-0629.

Bachynski, E. E., Moan, T., (2013), "Hydrodynamic modelling of tension leg platform wind turbines", In 32nd International Conference on Ocean, Offshore and Arctic Engineering, Nantes, France no. OMAE2013-10120.

Bachynski, E. E., (2014), "Design and Dynamic Analysis of Tension Leg Platform Wind Turbines", Ph.D. thesis, Norwegian University of Science and Technology Engineering Science and Technology Marine Technology.

Bae Y. H., Kim M. H., Im S. W., (2012), "Effects of Tower Elasticity and Aero-Loading in Aero-Elastic-Control-Floater-Mooring Coupled Dynamic Analysis for a TLP-type FOWT", Proc 22nd Int Offshore and Polar Eng Conf, Rhodes, ISOPE, Vol 1, pp 324–329.

Babarit A., Laporte-Weywada P., (2009), "On the Numerical Modelling of the Non Linear Behaviour of a Wave Energy Converter" Proceedings of the ASME 28th International Conference on Ocean, Offshore and Artic Engineering, Hawaii.

Bayati, I., Jonkman, J., Robertson A., Platt A., (2014), "The effects of second-order hydrodynamics on a semisubmersible floating offshore wind turbine". The Science of Making Torque from Wind 2014 (TORQUE 2014). Journal of Physics: Conference Series 524.

Bredsmose H., Mariegaard J., Paulson B. T., Jensen B., Schlør S., Larsen T. J., Kim T., Hansen A. M., (2013), " The Wave Loads Project". DTU Wind Energy Report E-0045.

Buchner , B., Forristall, G., Ewans, K., Christou, M., Hennig, J., (2011), "New insights in extreme crest height distributions (A summary of the Crest JIP)," Proc. 30th ASME International Conference on Offshore Mechanics and Arctic Engineering, Rotterdam, The Netherlands.

Bossler. A., (2011), " Floating Offshore Wind Foundations: Industry Projects in the USA, Europe and Japan". Maine Consulting, Inc. Technical Report.

Chakrabarti, S. K., (1987), "S.K. (1987) "Hydrodynamics of Offshore Structures". WIT Press.

DNV-RP-C205, (2010), "Recommended Practice. Environmental Conditions and Environmental Loads",124pp.

DNV-OS-J103, (2013), "Design of Floating Wind Turbine Structures", Det Norske Veritas AS: Hovik, Norway.

Duarte T., Sarmento A. JNA,Jonkman J., (2014), "Effects of Second-Order Hydrodynamic Forces on Floating Offshore Wind Turbines". Proc. of AIAA SciTech 2014, National Harbour, Maryland.

Engsig-Karup, A. P., Bingham, H. B., & Lindberg, O., (2009), "An efficient flexible-order model for 3D nonlinear water waves". Journal of Computational Physics, 228(6), 2100-2118. 10.1016/j.jcp.2008.11.028

Faltinsen, O. M., Newman, J. N., and Vinje, T., (1995), "Nonlinear Wave Loads on a Slender Vertical Cylinder," J. Fluid Mech., 289, pp. 179–198.

Fenton, J. D., (1988), "The numerical solution of steady water wave problems", Computers and Geosciences 14, 357-368.

Forristall, G. Z., (2000), "Wave Crest Distributions: Observations and Second Order Theory". Journal of Physical Oceanography. Vol. 30, 1931-1943.

Fossen, T. I., (2011), "Handbook of Marine Craft Hydrodynamics and Motion Control". John Wiley & Sons. 596 pages.

Fowler, M. J., Kimball, R. W., Ill, D. A. T., Goupee, A. J., (2013), " Design and testing of scale model wind turbines for use in wind/wave basin model tests of floating offshore wind turbines". In 32nd International Conference on Ocean, Offshore and Arctic Engineering, Nantes, France no. OMAE2013-10122.

Goupee A. J., Koo B., Kimball R. W., Lambrakos K. F., Dagher H. J., (2012), "Experimental comparison of three floating wind turbine concepts", Proceedings of the 31st ASME International Conference on Offshore Mechanics and Arctic Engineering, Rio de Janeiro, Brazil, 2012.

IEC, (2009), 61400-3, Ed.1, February – Wind Turbines Part 3: "Design requirements for offshore wind turbines".

Jonkman J., Butterfield S., Musial W., Scott G., (2009), "Definition of a 5MW reference Wind Turbine for Offshore System Development". NREL. 75pp.

Jonkman, J. M. and Buhl, Jr., M.L., (2005), "FAST User's Guide," NREL/TP-5000-38230. Golden, CO: National Renewable Energy Laboratory.

Journeé J. M. J., Massie W. W., (2001), "Offshore Hydromechanics", Delft University of technology, 1st Edition.

Kim, H. C., (2008). Nonlinear Waves and Offshore Structures. Advanced Series on Ocean Engineering – Volume 27. World Scientific.

Kimball, R., Goupee. A., Coulling A., Dahger, H., (2012), "Model Test Comparisons of TLP, Spar-buoy and Semi-Submersible Floating Offshore Wind Turbine Systems", SNAME Annual Meeting, October, 2012.

Lee, C., Newman, J., (2006), "WAMIT User Manual". Chestnut Hill, MA: WAMIT Inc.

Matha, D., (2009), "Model Development and Loads Analysis of an Offshore Wind Turbine on a Tension Leg Platform, with a Comparison to Other Floating Turbine Concepts", MSc Thesis. University of Colorado-Boulder.

Myrhaug, D., Kjeldsen, S. P., (1986), "Steepness and asymmetry of extreme waves and the highest waves in deep water". Ocean Engineering, Vol. 13, No.6. pp. 549-568..

Morison, J. R., O'Brien, M. P., Johnson J. W., Schaff, S. A., (1950), "The forces exerted by surface waves on piles", Pet. Trans., 189.

Naess A., Moan T., (2013), " Stochastic Dynamics of Marine Structures", Cambridge University Press.

Naess A., Stansberg C.T., Batsevych O., (2012), "Prediction of Extreme Tether Tension for a TLP by AUR and ACER Methods," J. of Offshore Mechanics and Arctic Eng., 134, DOI: 10.1115/1.4004954.

Ochi, M. K. (2003), "Hurricane-Generated Seas", 140 pp., Elsevier, New York.

Ogilvie, T. F., (1983), "Second-order hydrodynamic effects on ocean platforms", International Workshop on Ship and Platform Motions, Berkeley.

Øye, S., (1996), "Flex4 simulation of wind turbine dynamics", 28th IEA Meeting of Experts Concerning State of the Art of Aeroelastic Codes for Wind Turbine Calculationsn (available through International Energy Agency).

Paulsen, B. T., (2013), "Efficient computations of wave loads on offshore structures", Ph.D. thesis, The Technical University of Denmark, Department of Mechanical Engineering.

Philippe M., Courbois, A., Babarit, A., Bonnefoy, F., Rousset J.-M., Ferrant, P., (2013), " Comparison of simulation and tank test results of a semi-submersible floating wind turbine under wind and wave loads". In 32nd International Conference on Ocean, Offshore and Arctic Engineering, Nantes, France no. OMAE2013-11271.

Pinkster, J. A. Huijsmans, R. H., (1992), "Wave drift forces in shallow water". Geotechnology; Marine Transportation. British Maritime Technology.

Prowell, I., Robertson, A., Jonkman, J., Stewart, G.M., Goupee, A.J., (2013), "Numerical Prediction of Experimentally Observed Behaviour of a Scale-Model of an Offshore Wind Turbine Supported by a Tension-Leg Platform", Offshore Technology Conference, Houston, Texas, USA, May, 2013.

Puche, F. V. (2014), "Semi-submersible topside conceptual design: transition piece". MSc Thesis Aalborg University.

Rienecker, M.M. and Fenton, J.D., (1981), "A Fourier approximation method for steady water waves", J. Fluid Mech. 104, 119-137.

Roald L., Jonkman J., Robertson A., Chokani N., (2013), "The Effect of Second-Order Hydrodynamics on Floating Offshore Wind Turbines", Proc. DeepWind, Trondheim, Norway.

Robertson, A.N., Jonkman, J.M., Goupee, A.J., Coulling, A.J., Prowell, I., Browning, J., Masciola, M.D., Molta, P., (2013), "Summary of conclusions and recommendations drawn from the DeepCWind scaled floating offshore wind systems test campaign" , Proc. 32nd ASME International Conference on Offshore Mechanics and Arctic Engineering, Nantes, France.

Robertson A.,Jonkman J.,Vorpahl F., Popko W., Qvist J, Frøyd L., Chen X., Azcona J., Uzunoglu E., Soares C., Luan C., Yutong H., Pengcheng F., Anders Yde A., Larsen T., Nichols J., Builds R., Lei L., Nygaard T., Manolas D., Heege A., Ringdalen Vatne S., Ormberg H., Duarte1 T., Godreau C., Hansen H., Nielsen A., Riber H., Le Cunff C., Beyer F., Yamaguchi A., Jin Jung K., Shin H., Shi W., Park H., Alves M., Guérinel M., (2014), " OFFSHORE CODE COMPARISON COLLABORATION CONTINUATION WITHIN IEA WIND TASK 30: PHASE II RESULTS REGARDING A FLOATING SEMISUBMERSIBLE WIND SYSTEM", Proc. 33rd ASME International Conference on Ocean, Offshore and Arctic Engineering, San Francisco, California, USA.

Stansberg, C. T., (1997), "Comparing Ringing Loads From Experiments With Cylinders of Different Diameters - An Empirical Study," Proceedings 8th International Conference on Behaviour of Offshore Structures (BOSS'97), J. H. Vugts, ed., Elsevier, New York.

Thiagaran K.P., Dagher H.J., (2014), "A review of Floating Platform Concepts for Offshore Wind Energy generation". Journal of Offshore Mechanics and Arctic Engineering. Vol 136.

Utsunomiya, T., (2013), "At Sea Experiment of a Hybrid Spar for a Floating Offshore Wind Turbine Using a 1/10-Scale Model". Journal of Offshore mechanics and Arctic Engineering. Vol. 135.

Wehmeyer, C., Skourup J., Frigaard P. B., (2012), "Generic Hurricane Extreme Sea State. An engineering approach", Proc 22nd Int Offshore and Polar Eng Conf, Rhodes, ISOPE.

Wehmeyer, C., Ferri, F., Skourup J., Frigaard P. B., (2013), "Experimental Study of an Offshore Wind Turbine TLP in ULS Conditions", Proc 23rd Int Offshore and Polar Eng Conf, Anchorage, AK, ISOPE.

Wehmeyer, C., Ferri, F., Andersen M. T., Pedersen R. R., (2014),"Hybrid Model Representation of a TLP including flexible topsides in non-linear regular waves", Energies 2014, 7, 5047-5064; doi:10.3390/en7085047.

Wehmeyer, C., Rasmussen J. H., (2014), "Mooring responses of a floating offshore wind turbine in non-linear irregular waves", Journal of Ocean and Wind Energy (JOWE) 2014, (in review).